1-1-2014

Weak Decay Studies From An Effective Theory Standpoint

Aditya Yechan Gunja
Wayne State University,

WEAK DECAY STUDIES FROM AN EFFECTIVE THEORY STANDPOINT

by

ADITYA YECHAN GUNJA

DISSERTATION

Submitted to the Graduate School

of Wayne State University,

Detroit, Michigan

in partial fulfillment of the requirements

for the degree of

DOCTOR OF PHILOSOPHY

2014

MAJOR: PHYSICS

Approved by:

_____

Advisor   Date

_____

_____

_____

DEDICATION

To my dear little Lyre bird, for making this all worth it, always and forever

And for my grandparents, who were my first teachers, and the reason I'm here

ACKNOWLEDGMENTS

TABLE OF CONTENTS

LIST OF TABLES

LIST OF FIGURES

CHAPTER 1

INTRODUCTION

1.1 The Standard Model

The Standard Model (SM) of particle physics is the relativistic quantum field theory describing the fundamental particles that make up the Universe and their interactions [1, 2, 3]. The SM consists of the fundamental particles that make up matter. These include the 6 quarks (u, d, s, c, b, t) and 6 leptons $(e, \mu, \tau$ and the corresponding lepton neutrinos $\nu_e, \nu_\mu, \nu_\tau)$), which are fermions carrying half-integer spins. In addition there are spin 1 gauge bosons which act as the force carriers that mediate the two interactions; electroweak (EW) and quantum chromodynamics (QCD). The photon γ mediates electromagnetism, the $W^\pm$ and Z^0 mediate weak interactions and the gluons g mediate strong interactions. The recent crowning achievement in particle physics has been the discovery of a spin 0 Higgs boson that further solidifies the validity of the Standard Model. These fundamental particles make up all the "visible matter" in the observable universe and the forces arise from their interactions. Composite fermionic particles made up of 3 quarks are called baryons (e.g. neutron), and composite bosonic particles made up of a quark and an antiquark are called mesons(e.g. B meson).

Our description of particle physics is built out of gauge theories and the interactions are governed by gauge symmetries. Electromagnetic interactions couple to weak interactions and satisfy a local $SU(2)_L \times U(1)$ symmetry. The vector gauge bosons mediating these interactions make up the three W_i bosons and the weak hypercharge B-field. QCD is the theory describing the strong interactions of quarks and is governed by a local $SU(3)$ symmetry. The eight generators for this symmetry give rise to the gluons that are gauge bosons mediating
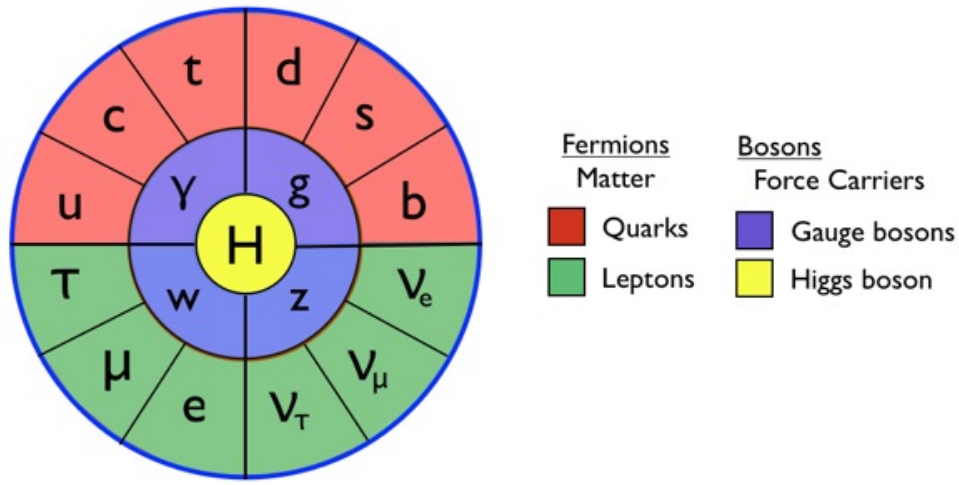
Figure 1.1.1: Particles of the standard model

the strong interactions.

Noether's Theorem demands that for every symmetry there exists a conserved current associated with the respective generator of the symmetry group. For example, the conservation of the current in the $U(1)$ gauge symmetry gives rise to electromagnetic charge, while the $SU(3)$ symmetry generates the "color" charge. Empirically the gauge bosons mediates weak interactions are found to have a mass as shown in Table 1.1.1. Mass terms for vector bosons can not be added to the Lagrangian while satisfying gauge invariance in the same way that they can be for fermions. So this is instead provided by Spontaneous Symmetry Breaking (SSB). The idea developed by three independent groups, Brout and Englert; Higgs; and Guralnik, Hagen and Kibble [4, 5, 6] which is commonly known as the Higgs mechanism provides a way to induce spontaneous breaking of the electroweak $SU(2) \times U(1)$ gauge symmetry. When a local symmetry is spontaneously broken the gauge field becomes massive and the goldstone boson is "eaten" to turn into the additional physical degree of freedom of the massive gauge field. It causes the original $U(1)$ gauge boson and three W_i bosons to mix into the photon and the massive electroweak $W^{\pm}$ and Z^0 bosons. A byproduct of this is the

recently discovered scalar Higgs boson.

Boson	Symbol	Mass (GeV)	Charge
photon	A^μ	0	0
gluon	g	0	0
Z Boson	Z^0	91.188	0
W Boson	$W^\pm$	80.385	± 1
Higgs Boson	H	≈ 125	0

Table 1.1.1: Properties of Standard Model Bosons

The leptons and quarks obtain masses through Yukawa interactions with the Higgs field. These come in three generations possessing the same quantum numbers but with varied masses. Their properties are listed in Table 1.1.2.

Particle	Symbol	Mass (MeV)	Charge (e)
up quark	u	$2.3^{+0.7}_{-0.5}$	2/3
down quark	d	$4.8^{+0.7}_{-0.3}$	$-1/3$
electron	e	0.510999	-1
electron neutrino	ν_e	≈ 0	0
charm quark	c	$1,275 \pm 25$	2/3
strange quark	s	95 ± 5	$-1/3$
muon	μ	105.658371	-1
muon neutrino	ν_μ	< 0.17	0
top quark	t	$(175.5 \pm 0.6 \pm 0.8) \times 10^3$	2/3
bottom quark	b	4180 ± 30	$-1/3$
tau lepton	τ	$(1,776.82 \pm 0.16)$	-1
tau neutrino	ν_τ	< 15.5	0

Table 1.1.2: Properties of Standard Model Fermions

Despite the standard models remarkable successes in describing phenomena within its domain and its accuracy in predictions of a variety of experiments, it is nevertheless incomplete. There are still several unanswered questions that may require modifications to the

SM, in order to be explained. Some of these questions include the nature of dark matter, the hierarchy problem and matter dominance over antimatter.

1.2 Quantum Chromodynamics

QCD is a local non-Abelian gauge theory describing the strong interaction of quarks. The gluons are mediators of these interactions and they come in eight color charges that are generators of the $SU(3)_c$ symmetry. The color-charged quark fields are invariant under transformations

$$q \rightarrow e^{i\lambda^i}q, \tag{1.1}$$

with λ^i being the generators of the gauge group.

The QCD Lagrangian is written as

$$\mathcal{L}_{QCD} = \bar{q}_f(i\gamma^\mu \mathcal{D}_\mu - m_q)q_f - \frac{1}{4}G^a_{\mu\nu}G^{a\mu\nu}, \tag{1.2}$$

where the flavor of quark q is denoted by f and repeated indices are summed over as usual. The color covariant derivative given by

$$\mathcal{D}_\mu = \partial_\mu - \frac{i}{2}g_s\lambda^i G^i_\mu, \tag{1.3}$$

contains λ^i, which are the eight generators of $SU(3)$, and G_μ is the gluon field. The gluons that act as the mediating gauge bosons are massless since QCD is an unbroken symmetry in the standard model.

We can define the QCD fine structure constant $\alpha_s = \frac{g_s^2}{4\pi}$. If the coupling constant is a small parameter, we can expand our theory perturbatively in order to obtain the matrix element for a transition. Applying this concept to the strong interactions is referred to as

Perturbative QCD (pQCD). In general every perturbative contribution can be described by Feynman Diagrams which are sets of topological diagrams for which amplitudes can be constructed using the Feynman rules derived from the Lagrangian.

Diagrams that are higher order in the coupling involve loops. In these the loop momenta are virtual, and are internally integrated over the entire range of momentum. This sometimes leads to divergences in the ultra-violet or infra-red limits. The process that we undertake in an effort to remove such divergences is called renormalization [7], through which the divergences are swept away by redefining masses and coupling constants to include both the "bare" parts from the original Lagrangian, as well "counter-terms" to the divergent pieces. This causes "running" of the coupling constant, which means a dependence of the coupling on the renormalization scale at which higher-order terms are absorbed,

$$Q^2 \frac{\partial \alpha_s\left(Q^2\right)}{\partial Q^2} \quad = \quad \beta\left(\alpha_s\right). \tag{1.4}$$

The β function drives the energy dependance and is a power series in α_s with $\beta(\alpha_s) = -\alpha_s^2(b_0 + b_1\alpha_s + b_2\alpha_s^2 + ...)$, where b_i depends on the number of particles involved in the loops at a given scale. Solving this renormalization group equation (RGE) provides the Q^2 dependence of our theory,

$$\alpha_s\left(Q^2\right) \quad = \quad \frac{\alpha_s(\mu^2)}{1 + b_0\,\alpha_s(\mu^2)\log\frac{Q^2}{\mu^2} + \mathcal{O}(\alpha_s^2)}. \tag{1.5}$$

In QCD the value of the leading order (1-loop) beta-function coefficient, b_0 is

$$b_0 \quad = \quad \frac{11C_A - 2n_f}{12\pi}, \tag{1.6}$$

where the first term $C_A = 3$ is due to the $SU(3)$ gluon loop virtual corrections. The second term is due to quark loops with n_f being the number of active quark flavors that are

considered to be light, having mass less than Q^2. In the standard model which contains a maximum of 6 flavors this means $b_0 = \frac{7}{4\pi}$. If we look at processes involving large momentum transfers, the value of the coupling constant evaluated at the weak scale is

$$\alpha_s(m_Z) \quad = \quad 0.1184(7). \tag{1.7}$$

This allows us to extrapolate at a different scale, for example,

$$\alpha_s(m_D) \quad = \quad 0.3039. \tag{1.8}$$

The negative overall sign in the expansion of β combined with the fact that $b_0 > 0$ (for $n_f \leq 16$) is the origin for the positive nature of the term in (1.5). This means that the coupling decreases with increasing energy scale, which is known as Asymptotic Freedom [8]. Conversely, as we go towards smaller energies, in the limit that $Q^2 \to \Lambda$ (where Λ, the Landau pole, is a constant of integration when solving (1.5) up to leading order) we can see that the coupling constant would rapidly diverge. The most striking consequence to this is that below 1 GeV, the coupling constant is no longer a good parameter for expansion. This is the around the energy where confinement permits hadrons, bound states of QCD partons, to be formed and we must look towards other phenomenological methods to describe the dynamics involving them.

So while a perturbative approach to QCD works in the high energy regime (much greater than $\Lambda_{QCD} \sim 200$ MeV), in low energy theory we must deal with non-perturbative effects as well, which can pose some complications. One way of tackling such calculations is to identify natural factorization scales contained in the specific problem that can split our theory into multiple energy regions. For example, the heavy quarks contained in some mesons (like charm or bottom), provide a natural scale with which to calculate the perturbative effects and separate out "hard" physics and "soft" physics.

A puzzling feature contained in QCD is that although it allows for violation of CP-symmetry in strong interactions experiments do not indicate any CP violation in the QCD sector. This is one of the big open fine tuning issues and is posed as the strong CP problem. In order to resolve this the Peccei and Quinn postulated an additional global symmetry to the standard model (called the Peccei-Quinn symmetry)[9]. Spontaneous breaking of this symmetry leads to the existence of a new pseudoscalar particle called the axion [10, 11]. As we shall see later, particles such as these come in handy to provide candidates for dark matter.

1.3   Dark Matter

An area of physics beyond the standard model that I shall discuss is the open question on the nature of dark matter (DM). We believe it accounts for about 26.8% of the observable universe beyond the visible matter that makes up the stars and galaxies and is particulate in nature [12, 13]. The evidence for dark matter comes from a variety of cosmological sources like the rotation curves of galaxies [14], features of the cosmic microwave background fluctuation spectrum [15], gravitational lensing [16],and large scale cosmological structures [17]. The dark matter accounts for the majority of mass in our universe and the evidences all point towards a density for dark matter that is many times that of visible matter.

To take one example, cosmological observations of the galactic rotation velocity distribution do not conform to gravitational predictions based on the apparent visible mass of the observed galaxy as shown in Fig 1.3.1. The distribution seen gives cause to believe there is a large amount of invisible matter in the universe, distributed in halos around galaxies.

The nature of this dark matter is still a mystery as this kind of data only probes its gravitational interaction. So DM is one of the major drivers for research in current astro-particle physics. There are no particles in the SM that can account for the amount of mass
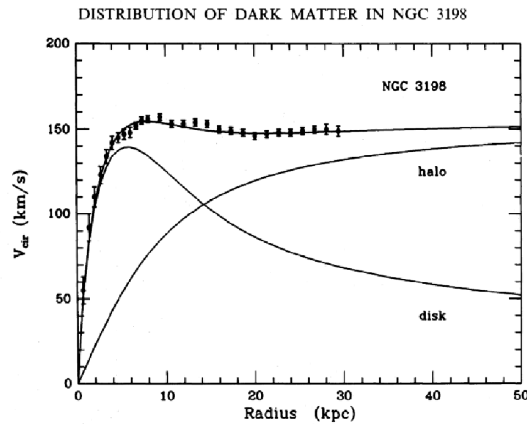
Figure 1.3.1: Rotation Velocity Distribution of Galaxies

deduced, and studying its non-gravitational interactions is a primary experimental focus in colliders, underground detectors and astrophysics. There are significant theoretical efforts to model possible scenarios of DM, and many experiments [18, 19] have been proposed, built and completed with significant results constraining the cross-sections and masses of DM candidates through direct detection.

One of the most popular models for dark matter is of a weakly interacting particle with a mass set around the electroweak scale. This is motivated by a thermal mechanism for populating the universe with dark matter with a relic abundance. Experimental measurements of the abundance $\Omega_{DM}h^2 \sim 0.12$ by WMAP collaboration [20] can be used to place constraints on the masses and interaction strengths of those DM particles. It implies a relation

$$\Omega_{DM}h^2 \sim \langle \sigma_{ann}v_{rel} \rangle^{-1} \propto \frac{M^2}{g^4},$$

with M and g being the mass and the interaction strength associated with DM annihilation. This in turn requires a specific annihilation cross section that can be provided by a weakly interacting particle with a mass set around the electroweak scale, which therefore leads to the prevailing WIMP paradigm for cold dark matter. However, there is motivation for

studying models of light dark matter with masses in the keV range. The light mass implies a superweak interaction between the dark matter and SM sector which will be discussed in Chapter 5.

1.4   Weak Decays and Flavor Physics

Electroweak decays of bound-state hadrons are of particularly useful to test the standard model and to search for any new physics since some of these decay channels are quite rare. New physics could appear at high energies and we can expect that it would show itself in rare processes and would be associated with low decay widths. It is therefore crucial to get a firm grip on on the standard model calculations in these processes and their SM backgrounds in order to pin down any new physics hiding there and thereby obtain precision tests for our current theories. For example some experimentally clean processes such as leptonic decay of heavy mesons are suppressed in the standard model, and we shall focus on some of these in the following chapters.

Recently, B-physics has been a very lucrative sector for the study of heavy meson dynamics. With the B-factories (such as Belle at KEK, BaBar at SLAC, CDF at Fermilab and LHCb at CERN) there is a large amount of experimental data available to help test predictions of the standard model. While current data shows little deviation in physics predicted by the SM it is important to analyze any discrepancies in rare B decays leaving room for the discovery of new physics. These decays provide a lot of useful information as they contain parameters involved in both: electroweak currents and interactions (such as CKM matrix elements and meson decay constants), as well as strong interaction dynamics required in the formation of mesons in terms of their constituent bound quarks. We discuss two such classes of meson decays in the following work.

Firstly we consider leptonic decays of charged mesons such as the $B^{\pm}$ (which has a mass
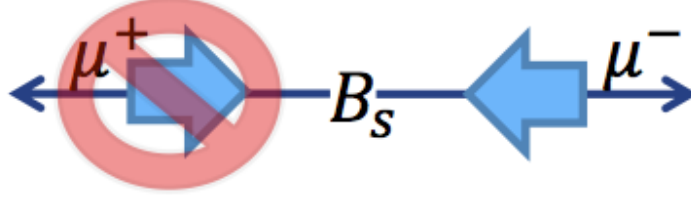
Figure 1.4.1: Helicity suppression

of about 5280 MeV). Experimentally upper limits are found for the branching ratio of the electron and muon channels whereas the tau channel is observed

$$\mathcal{B}r(B^\pm \to e^\pm \bar{\nu}_e) \quad < \quad 9.8 \times 10^{-7}, \tag{1.9}$$

$$\mathcal{B}r(B^\pm \to \mu^\pm \bar{\nu}_\mu) \quad < \quad 1.0 \times 10^{-6}, \tag{1.10}$$

$$\mathcal{B}r(B^\pm \to \tau^\pm \bar{\nu}_\tau) \quad = \quad (1.64 \pm 0.34) \times 10^4. \tag{1.11}$$

This stems from a particular feature of leptonic decays of pseudoscalar mesons. The decay width for these processes are helicity suppressed by a factor of $(m_\ell/m_P)^2$. This is because the initial meson is spinless and a helicity flip on an external lepton line is required to conserve angular momentum. In the standard model, weak interactions involve only left handed currents and the lepton and neutrino (or two leptons) that are emitted in opposite directions tend to have the same spin configuration. This violates angular momentum in the massless limit and is therefore suppressed by the mass of the lepton. The suppression can in fact be lifted with the addition of a unit of angular momentum in the form of a third particle in the final state that carries spin or a p-wave.

We shall utilize this aspect in our calculations when a third particle such as a photon or a dark matter candidate are coupled to these decays. Theoretically the phase space distribution for such two body decays is a delta function, but experimentally it is smeared out and we get a spread. We can then constrain parameters in the region coinciding with the disparate three body spectrum.
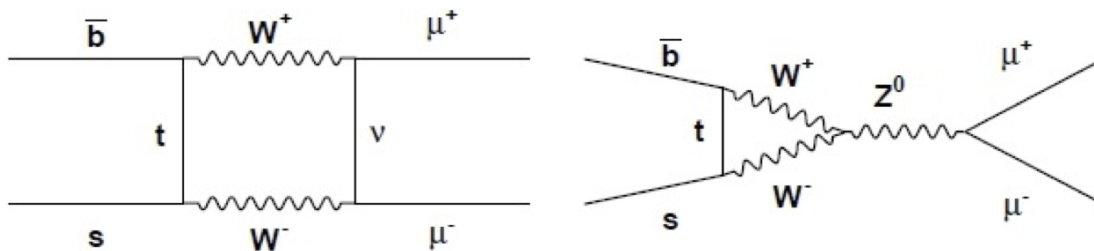
Figure 1.4.2: One-loop diagrams contributing to $B_s \to \mu^+\mu^-$

Next we also look at the di-muonic decay of the neutral B_s^0 meson. This is an example of a decay that contains flavor changing neutral currents (FCNC), where the quark changes into a quark of different flavor but the same charge $(b \to (s,d), c \to u)$. It is very rare so its rate could be severely affected by new physics. FCNC's don't exist in the standard model at tree-level and they only occur through loop diagrams such as the box and penguin diagrams shown in Fig 1.4.2. Therefore they are difficult to produce in the SM and could provide a powerful way to discover new physics. We focus on calculating backgrounds to this decay in the standard model with the addition of soft photons and missing energy.

Additionally, we look at the exclusive weak decay of the W radiatively into a Pseudoscalar (P), such as a Pion, and a photon. Electroweak and strong interaction dynamics can be probed in the standard model using these decays and we discuss this in Chapter 4. From a particular perspective this decay is essentially similar to a mirror image of a charged meson decay (without a final state lepton current).

1.5 Model Independent Approach

In our calculations, we avoid using particular theoretical models in order to describe and verify the dynamics at the various energy scales. Our philosophy is to adopt a more general phenomenological approach to tackle each situation by using effective Lagrangians

and currents which are consistent with the fundamental symmetries that would describe the physics at the relevant scales. We do this by employing effective field theories (EFT). The purpose of this method is to represent the dynamical content of a theory in the low energy limit and factor out the effects of heavy particles into a few constants. We can usually find natural scales associated with the problem through relevant masses or interaction energies, and we can use these to construct some small parameter with which to set up a perturbative expansion. For instance if there are particles involved with vastly separated masses like light pions and heavy quarks, we can invoke two scales, one light and one heavy. The light scale is where QCD becomes strongly coupled, Λ_{QCD}, so that perturbation theory breaks down and nonpertubative strong interaction effects dominate. Hadron masses such as light meson mass are expressed as dimensionless multiples of Λ_{QCD} which experimentally is ~ 200 MeV. Additionally we have a heavy scale such as the heavy quark mass m_Q. So we can expand the theory in orders of $\frac{\Lambda_{QCD}}{m_Q}$ where small parameters are involved, such as a light quark mass or specific projections of momenta ("collinear" or "transverse") which are smaller than or of the order of Λ_{QCD}.

When we study the physics of a process at some energy scale E we take into account all the particles that can be produced at that energy, but there are fields which are too heavy to be directly produced. These are only involved through virtual effects and we don't include them in the Lagrangian when describing the effective low energy theory. Their virtual effects are incorporated into various couplings between light fields and this process of removing heavy fields is known as "integrating out the fields". We find a simple example of this in electroweak current interactions that we encounter in phenomena such as the weak decays described in this dissertation.

Mesonic weak decays are executed through the weak decays of their constituent quarks. A four fermion electroweak interaction is mediated by the exchange of a massive W boson at tree level in the full Weinberg-Salam theory. The W boson couples to vector and axial
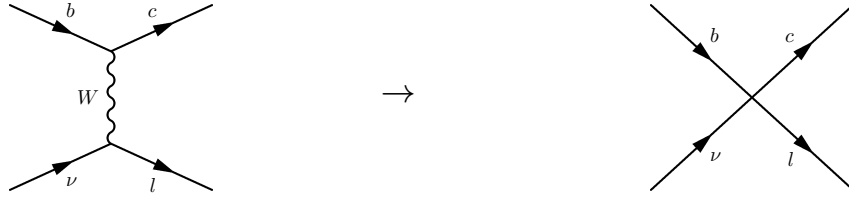
Figure 1.5.1: Fermi theory for four-quark weak interaction

vector quark currents of the form

$$(q_1\bar{q}_2)_{V-A} \quad = \quad q_1\gamma_\mu(1-\gamma^5)\bar{q}_2. \tag{1.12}$$

Including the weak couplings, the amplitude for the tree level diagram shown in the left of Fig. 1.5.1 is

$$\mathcal{A}(bc \to \ell\nu) \quad = \quad \left(\frac{g}{\sqrt{2}}\right)^2 V_{cb}\,[\bar{c}\gamma_\mu P_L b]\,\frac{-i\left(g^{\mu\nu}-\frac{P^\mu P^\nu}{M_W^2}\right)}{P^2-M_W^2}\,[\bar{\nu}\gamma_\nu P_L \ell], \tag{1.13}$$

where $P_L = \frac{1}{2}(1-\gamma^5)$.

At energies less than the electroweak scale $\mathcal{O}(M_{Z,W} \approx 80 - 90 GeV)$ we can simplify the physics into an effective four-fermion point interaction because the gauge boson is heavy. Since $P \ll M_W$ we can apply this approximation to simplify the W boson propagator and expand in their ratio of these quantities so that

$$\frac{-i\left(g^{\mu\nu}-\frac{P^\mu P^\nu}{M_W^2}\right)}{P^2-M_W^2} \sim \frac{-i}{M_W^2} + \mathcal{O}\left(\frac{P^2}{M_W^2}\right). \tag{1.14}$$

Therefore the low energy limit of electroweak theory leads to the Fermi theory of weak interactions [21], which is described by the local effective hamiltonian

$$\mathcal{H}_{eff} \quad = \quad i\frac{G_F}{\sqrt{2}}V_{cb}\,(\bar{c}b)_{V-A}\,(\bar{\nu}\ell)_{V-A}, \tag{1.15}$$

where the Fermi constant is defined by

$$\frac{G_F}{\sqrt{2}} = \frac{g^2}{8M_W^2}.$$ (1.16)

This gives us the basic idea of an operator product expansion (OPE), where one represents the low energy effects from a heavy sector of the theory by employing an effective Lagrangian that is expanded as a series of local operators having the symmetries of the theory and weighted by effective coupling constants called Wilson coefficients. In the above example the Wilson coefficients is 1 since there are no scale dependent couplings and the W boson is integrated out and is no longer a dynamical degree of freedom. In general we can write,

$$\mathcal{L}_{eff} = \sum_i C_i(\mu)\mathcal{O}_i.$$ (1.17)

The Lagrangian always has mass dimension 4, so if an operator has a dimension d the coefficient must have mass dimension of $C_i \sim M^{4-d}$ where the mass scale is associated with the heavy sector of the theory. We can see then that operators of high dimension will be suppressed by powers of the heavy mass. The Wilson coefficients C_i, can be calculated by matching the effective theory with the full theory at any required order in the the perturbative expansion. Of course, one of the common and most important uses of effective field theory is to parametrize the way that new physics at high energies can affect low energy observables.

This dissertation is organized as follows. We shall discuss a few problems involving weak decays that we have worked on where we employ this model independent approach. To set the framework for many of the calculations that we undertake we shall discuss some of the Effective field theory techniques that we employ in Chapter 2. We shall then begin in Chapter 3 with a standard model calculation involving the soft photon contribution to leptonic B decays and ways in which to deal with possible contamination to the popular rare decay channel $B_s \rightarrow \mu^+\mu^-$. We shall utilize heavy quark and chiral symmetries that are

relevant to the scales in the problem and work with them in heavy meson chiral perturbation theory. Chapter 4 will continue with another weak decay in the standard model involving an analysis of Exclusive W decays in pQCD and EFT. We shall see that the kinematics involved in these decays shall point towards soft collinear effective theory as the useful framework for calculation. We then move onto some new physics in Chapter 5 by studying the application of leptonic meson decays in constraining parameters relating to a couple of general candidates of light dark matter in a model independent way.

CHAPTER 2

EFFECTIVE FIELD THEORIES

2.1   Heavy Quark Effective Theory

We saw that the QCD Lagrangian from Eq. (1.2) describes the strong interactions of light quarks and gluons and this dynamically generates a non-perturbative scale Λ_{QCD}. In the weak decays that we look at we wish to describe mesons that are color singlet states of a quark antiquark pair bound by non-pertubative gluon dynamics. Heavy mesons $Q\bar{q}$ in particular contain a heavy quark with a mass $m_Q \gg \Lambda_{QCD}$ and a light quark $m_q \ll \Lambda_{QCD}$. Since Λ_{QCD}^{-1} provides a typical scale for the size of this system it is a good approximation to take the $m_Q \to \infty$ limit of QCD where it exhibits spin-flavor heavy quark symmetry [22].

The momentum transfer between the heavy and light quarks arising from the dynamics is of the order of Λ_{QCD} and so the large mass of the heavy quark implies that its velocity is pretty much unchanged by these strong interaction effects. Therefore the heavy quark just acts as a static color source which the light degrees of freedom interact with, in the same spirit as any two body system with an approximate fixed infinite mass such as a proton in a hydrogen atom. The flavor of the heavy quark within the heavy meson then becomes irrelevant as they would interact the same way irrespective of their particular mass which goes to infinity in the approximation. This gives the *heavy quark flavor symmetry* since the dynamics is invariant under the exchange of heavy quark flavors. In the $m_Q \to \infty$ limit the heavy quark only interacts with the gluon chromoelectrically and is spin independent. The dynamics are unaffected by arbitrary transformations on the spin of the heavy quark and so we also gain *heavy quark spin symmetry*. Any breaking of the flavor symmetry (in the form of finite mass effects for heavy quarks of different masses) or of the spin symmetry (in the

form of chromomagnetic interactions of the heavy quark) would appear as $\mathcal{O}(1/m_Q)$ terms and will be NLO corrections to the theory. In the ground state the heavy quark and the light degrees of freedom composing the meson form a multiplet with spin 0 or 1. For the b quark case, these correspond to the B and B^* mesons respectively, and they are essentially degenerate in mass in the heavy quark limit.

To construct physical states using the above mentioned symmetries, we can formulate a covariant representation of fields where the entire multiplet of degenerate states is treated as a single object. We can use a matrix representation to define the field $H_a(x)$ that transforms linearly under heavy quark symmetries.

$$H_a = \frac{1+ \slashed{v}}{2}(P^*_{a\mu}\gamma^\mu - P_a\gamma_5), \tag{2.1}$$

where a is a light quark flavor index. The field is a linear combination of the pseudoscalar field $P_a(x)$ and the vector field $P^*_{a\mu}(x)$, (with a polarization vector ϵ_μ associated). It annihilates the meson doublet corresponding to the spin 0^- and spin 1^- states. Due to the static approximation, the heavy quark can be labelled by a four-veloctiy v that does not change with time. H_a and its conjugate field defined as $\bar{H}_a = \gamma^0(H_a)^\dagger\gamma^0$, both transform as bispinors under Lorentz transformations and it is possible to write down interactions that are invariant under the heavy quark symmetries using these fields.

We can then rewrite the QCD Lagrangian to manifestly display heavy quark spin-flavor symmetries as $m_Q \rightarrow \infty$ and replace it with an effective theory. This is known as heavy quark effective theory (HQET) and it describes the dynamics of mesons with a single heavy quark [23, 24]. If we consider an off-shell heavy quark interacting with external fields, its momentum can be separated into the static and dynamic parts

$$p_Q = m_Q v + k, \tag{2.2}$$

where k is the residual momentum that parametrizes the amount by which it is off-shell and is therefore of the order of Λ_{QCD}. Then the Dirac quark propagator simplifies to

$$i\frac{(\not{p}_Q + m_Q)}{p_Q^2 - m_Q^2} \rightarrow i\frac{(1+\not{v})}{2v \cdot k} + \mathcal{O}\left(\frac{k^\mu}{m_Q}\right). \tag{2.3}$$

We can extract this dominant part of the heavy quark momentum from the original QCD quark fields by factoring them into a large and small component

$$q(x) = e^{-im_Q v \cdot x}[Q_v(x) + \mathcal{Q}_v(x)] \tag{2.4}$$

$$\text{where} \quad Q_v(x) = e^{im_Q v \cdot x}\frac{(1+\not{v})}{2}q(x), \tag{2.5}$$

$$\text{and} \quad \mathcal{Q}_v(x) = e^{im_Q v \cdot x}\frac{(1-\not{v})}{2}q(x). \tag{2.6}$$

The large component field $Q_v(x)$ produces effects at the leading order, while the small component field $\mathcal{Q}_v(x)$ can be integrated out when deriving the effective Lagrangian since it produces effects of the order of $1/m_Q$. In contrast to the QCD Lagrangian, only inverse powers of m_Q would appear in the effective Lagrangian. The fields satisfy projection constraints

$$\not{v}Q_v = Q_v, \qquad \not{v}\mathcal{Q}_v = -\mathcal{Q}_v. \tag{2.7}$$

Substituting Eq. (2.4) into the QCD Lagrangian shows us that Q_v is massless and $\mathcal{Q}_v$ has a mass of $2m_q$. The non-local effective Lagrangian can be derived by integrating out the heavy field $\mathcal{Q}_v$ as shown in [25]. This is done by solving for its equation of motion to get $(iv \cdot D + 2m_Q)\mathcal{Q} = i\not{D}Q_v$ and reinserting it into the Lagrangian. The HQET Lagrangian is

$$\mathcal{L}_{HQET} = \bar{Q}_v(iv \cdot D)Q_v - \bar{Q}_v\frac{D^2}{2m_Q}Q_v - g\bar{Q}\frac{\sigma_{\mu\nu}G^{\mu\nu}}{4m_Q}Q_v + \mathcal{O}\left(\frac{1}{m_Q^2}\right), \tag{2.8}$$

where the first term gives the tree-level leading order Lagrangian in the $(1/m_Q)$ expansion.

2.2 Chiral Perturbation Theory

Now that we have dealt with heavy quarks, we can move on to the light quarks u, d and s whose masses are very small compared to Λ_{QCD}. Here we consider an approximation to QCD where the light quark masses vanish and we can do perturbation theory around m_q in this limit [26]. Chirality is defined by using the left and right projection operators $P_{L/R} = \frac{1}{2}(1 \mp \gamma^5)$ and the QCD Lagrangian can be expanded in terms of these as

$$\mathcal{L}_q = \bar{q}\left(i \not{D} - m_q\right)q = \bar{q}_L i \not{D} q_L + \bar{q}_R i \not{D} q_R - \bar{q}_L m_q q_R - \bar{q}_R m_q q_L. \tag{2.9}$$

We see that in the $m_q \to 0$ limit (where only the first two terms remain) the Lagrangian exhibits invariance under an $SU(3)_L \times SU(3)_R$ chiral symmetry. Under this symmetry the right handed and left handed quark fields transform differently as

$$q_L \to L q_L, \quad q_R \to R q_R, \tag{2.10}$$

where L and R are the respective unitary transformations of the groups. This is called the chiral limit in which we can do chiral perturbation theory (χPT). If $m_q \neq 0$ then there is a mass term

$$\bar{q}_L \, L^\dagger \, m_q \, R \, q_R - \bar{q}_R \, R^\dagger \, m_q \, L \, q_L \neq 0. \tag{2.11}$$

Since the quarks in fact have small masses in the SM the symmetry is spontaneously broken

by the vacuum expectation value of quark bilinears

$$\langle \bar{q}_R^j q_L^k \rangle = \lambda_0 \, \delta^{kj} \tag{2.12}$$

where j and k are flavor indices. If we make transformations in $SU(3)_L \times SU(3)_R$ transformations, those with $L = R$ leave the vacuum expectation value unchanged. So the symmetry is spontaneously broken to its diagonal subgroup $SU(3)_V$.

The Goldstone Bosons that arise from the broken generators form an octet and correspond to the light pseudoscalar particles π, K, $\bar{K}$, η which represent the low-energy long-wavelength excitations of $\bar{q}_R q_L$. These mesons acquire masses due to the explicit symmetry breaking. We can describe the Goldstone Boson fields by a 3×3 special unitary matrix Σ

$$\Sigma = \xi^2 = \exp\left(\frac{2iM}{f}\right), \tag{2.13}$$

where $f \approx 130$ MeV, and which transforms under $SU(3)_L \times SU(3)_R$ as

$$\Sigma \to L \, \Sigma \, R^\dagger. \tag{2.14}$$

Σ is the exponential of a Hermitian and traceless matrix which can be written out explicitly in terms of the eight Goldstone Boson fields

$$M = \begin{pmatrix} \frac{\pi^0}{\sqrt{2}} + \frac{\eta}{\sqrt{6}} & \pi^+ & K^+ \\ \pi^- & -\frac{\pi^0}{\sqrt{2}} + \frac{\eta}{\sqrt{6}} & K^0 \\ K^- & \bar{K}^0 & -\sqrt{\frac{2}{3}}\eta \end{pmatrix}. \tag{2.15}$$

To the lowest order in momentum, strong interactions of the Goldstone bosons are described

most generally by the invariant effective Lagrangian

$$\mathcal{L}_{eff} = \frac{f^2}{8} \text{Tr} \left[\partial^\mu \Sigma \partial_\mu \Sigma^\dagger \right] . \tag{2.16}$$

Higher order terms are suppressed by powers of p/Λ_χ where p is a typical momentum and Λ_χ is the chiral symmetry breaking scale ~ 1 GeV.

We can include the effects of quark masses on the strong interactions of the Goldstone Bosons by adding terms that transform the same way as the light quark mass terms from Eq. (2.9)

$$\sum_a \bar{q}_a \hat{m}_{ab} q_b, \tag{2.17}$$

where a and b are light quark flavors (u,d,s) and the diagonal light mass matrix is given by

$$\hat{m}_{ab} = \begin{pmatrix} m_u & 0 & 0 \\ 0 & m_d & 0 \\ 0 & 0 & m_s \end{pmatrix} . \tag{2.18}$$

We can take into account this symmetry breaking at first order in masses of the quarks by adding to the effective lagrangian to give

$$\mathcal{L}_\chi = \frac{f^2}{8} D_\mu \Sigma_{ab} D^\mu \Sigma_{ba}^\dagger + \lambda_0 \text{Tr} \left[\hat{m}\Sigma + \Sigma^\dagger \hat{m} \right] + \mathcal{O} \left((\partial\Sigma)^3 \right) + \mathcal{O} \left(\hat{m}^2 \right) . \tag{2.19}$$

The second term in the Lagrangian gives rise to the masses of π, K and η and are therefore

referred to as pseudo-Goldstone Bosons. For example

$$m_{\pi^{\pm}}^2 = \frac{4\lambda_0}{f^2}(m_u + m_d),$$

$$m_{K^{\pm}}^2 = \frac{4\lambda_0}{f^2}(m_u + m_s),$$

$$m_{K^0}^2 = \frac{4\lambda_0}{f^2}(m_d + m_s). \tag{2.20}$$

In order to describe the interactions of these Goldstone fields with matter fields such as heavy mesons, baryons or light vector mesons, chiral Lagrangians are typically written with a coset field $\xi(x)$ as defined in Eq. (2.13). The transformation law for matter fields involves only $U(x)$ which is a member of the unbroken $SU(3)_V$ subgroup. So it is useful to define ξ which has a transformation law involving U, L and R as discussed in [27]

$$\xi(x) \to L\xi(x)U^{\dagger}(x) = U(x)\xi(x)R^{\dagger}. \tag{2.21}$$

To construct invariant Lagrangian terms, it is useful to form covariant derivatives or gauge fields with combinations of ξ, and whose transformation laws involve only U. This is provided by

$$\mathcal{V}_{\mu} = \frac{1}{2}\left(\xi^{\dagger}\partial_{\mu}\xi + \xi\partial_{\mu}\xi^{\dagger}\right), \tag{2.22}$$

$$\text{and} \quad \mathcal{A}_{\mu} = \frac{i}{2}\left(\xi^{\dagger}\partial_{\mu}\xi - \xi\partial_{\mu}\xi^{\dagger}\right). \tag{2.23}$$

$\mathcal{V}_{\mu}$ has the quantum numbers of a vector field and $\mathcal{A}_{\mu}$ has the quantum numbers of an axial-vector field. Their transformation properties follow

$$\mathcal{V}_{\mu} \to U\mathcal{V}_{\mu}U^{\dagger} + U\partial_{\mu}U^{\dagger}, \tag{2.24}$$

$$\mathcal{A}_{\mu} \to U\mathcal{V}_{\mu}U^{\dagger}. \tag{2.25}$$

So we can use ξ to introduce electromagnetic interactions through a covariant derivative such as

$$\mathcal{D}_\mu \xi = \partial_\mu \xi + ieB_\mu[Q,\xi], \tag{2.26}$$

where $Q = \text{diag}\left[\frac{2}{3}, -\frac{1}{3}, -\frac{1}{3}\right]$ gives the charge.

2.3 Heavy Meson Chiral Perturbation Theory

We can now study to the implications of combining chiral and heavy quark symmetries to obtain heavy meson chiral perturbation theory (HχPT) in order to describe interactions of heavy mesons and pions, kaons etc [28].

As mentioned previously the doublet field H_a that is composed of the degenerate psuedoscalar and vector meson pair P and P^* transforms as an anti triplet under chiral transformations so that $H_a \rightarrow H_b U^\dagger_{ba}$. Knowing now the transformation properties of both the heavy and light fields, we can construct a Lorentz invariant H-field chiral Lagrangian that satisfies $SU(3)_L \times SU(3)_R$ and heavy quark symmetry as an expansion in $1/M$ where M is the H-field mass [29]. Just as in HQET scaling the heavy meson fields by $\exp(-iM\,v\cdot x)$ removes the mass term. This is equivalent to measuring energies relative to M rather than m_Q. At the leading order, the Lagrangian is

$$\mathcal{L}_{(0)} = -iTr\left[\bar{H}_a v_\mu (\partial^\mu \delta_{ba} + i\mathcal{V}^\mu_{ba})H_b\right] + gTr\left[\bar{H}_a H_b \gamma_\mu \gamma^5 \mathcal{A}^\mu_{ba}\right] + \frac{f^2}{8}D_\mu \Sigma_{ab}D^\mu \Sigma^\dagger_{ba}. \tag{2.27}$$

Heavy quark spin symmetry disallows the occurrence of gamma matrices between the $\bar{H}$ and H fields in the trace ("heavy quark side") and it can only occur on the right of H ("light quark side) in the trace in any combination. The kinetic terms in the Lagrangian give the

propagators

$$\frac{i}{2v \cdot k}, \qquad \frac{-i\left(g^{\mu\nu} - v^{\mu}v^{\nu}\right)}{2v \cdot k}, \tag{2.28}$$

for the P and P^* mesons respectively.

The first term in the Lagrangian of Eq.(2.27) that involves $\mathcal{V}^{\mu}$ contains an even number of psuedo-Goldstone fields, but the terms involving $\mathcal{A}^{\mu}$ contain an odd number of pseudo-Goldstone fields. These are proportional to g and will give us single light-meson couplings with the heavy mesons in the form of P^*P^*M and P^*PM interactions when expanded out

$$\mathcal{L}_{int} = \frac{2ig}{f} P_a^{*\mu\dagger} P_b \partial_{\mu} M_{ba} - \frac{2ig}{f} P_a^{*\mu\dagger} P_b^{*\nu} \partial^{\alpha} M_b a \epsilon_{\mu\beta\nu\alpha} v^{\beta} + h.c. \tag{2.29}$$

At leading order in $1/M$ the coupling constants are equal as a consequence of heavy quark symmetry and PPM does not exist due to parity considerations.

We can consider NLO contributions in the $1/M$ expansion by including effects that break chiral symmetry or heavy quark symmetry as corrections to the effective Lagrangian. The heavy quark spin symmetry violation appears as magnetic moment operators and can be taken into account by adding

$$
\begin{aligned}
\delta\mathcal{L}^{(1)} &= \frac{\lambda_2}{M} Tr[\bar{H}_a \sigma^{\mu\nu} H_a \sigma_{\mu\nu}] \\
&+ \frac{g_1}{M} Tr\left[H_b \gamma_{\mu} \gamma^5 \mathcal{A}_{ba}^{\mu} \bar{H}_a\right] \\
&+ \frac{g_2}{M} Tr\left[\gamma_{\mu} \gamma^5 \mathcal{A}_{ba}^{\mu} H_b \bar{H}_a\right].
\end{aligned}
\tag{2.30}
$$

The only effect of the first term in Eq.(2.30) is to give rise to a mass splitting between the P and P^* mesons

$$\Delta = M_{P^*} - M_P = -2\frac{\lambda_2}{M}. \tag{2.31}$$

The P and P^* propagators then get shifted to give

$$\frac{i}{2(v \cdot k + \frac{3}{4}\Delta)}, \qquad \frac{-i\left(g^{\mu\nu} - v^\mu v^\nu\right)}{2(v \cdot k - \frac{1}{4}\Delta)}. \tag{2.32}$$

The last two terms in Eq. (2.30) lead to corrections to the constant g for P^*P^* and PP^* interactions

$$g \to g_{P^*P^*} = g + \frac{1}{M}(g_1 + g_2)$$
$$g \to g_{PP^*} = g + \frac{1}{M}(g_1 - g_2). \tag{2.33}$$

Chiral symmetry is explicitly broken by the light quark mass matrix $\hat{m}_q$ and these effects at lowest order can be taken care of by adding

$$\delta\mathcal{L}^{(2)} = \lambda_1 Tr[\bar{H}_a H_b \hat{m}_{ab}^\xi] + \lambda_1' Tr[\bar{H}_a H_a \hat{m}_{bb}^\xi] \tag{2.34}$$

where $m^\xi = \left(\xi^\dagger \hat{m}\xi + \xi\hat{m}\xi^\dagger\right)$. The first term gives rise to mass differences in the heavy mesons due to $SU(3)_V$ breaking and the second term is an overall shift in meson masses due to light quark masses. Additionally we can introduce electromagnetic interactions using a contact term such that

$$\mathcal{L}_\beta = -\frac{\beta e}{4}Tr\left[H_b\sigma^{\mu\nu}F_{\mu\nu}Q_{ba}^\xi\bar{H}_a\right] - \frac{e}{4m_Q}Q_Q' Tr\left[\bar{H}_a\sigma^{\mu\nu}H_aF_{\mu\nu}\right], \tag{2.35}$$

where $Q^\xi = \frac{1}{2}\left(\xi^\dagger Q\xi + \xi Q\xi^\dagger\right)$ [30]. Interaction of a photon with the light degrees of freedom inside the heavy meson is described by the first term while the second term which is the electromagnetic interaction with the heavy quark is suppressed by $1/m_Q$. It could contribute to cancellation effects with one-loop corrections to transition amplitudes.

π_a $\qquad\qquad$ π_a $\qquad\qquad$ $= \frac{i}{p^2-m^2}$

P^*_b $\qquad\qquad$ P^*_a $\qquad\qquad$ $= \frac{i}{2(v\cdot k+\frac{3}{4}\Delta)}$

P^*_a $\qquad\qquad$ P^*_a $\qquad\qquad$ $= \frac{-i(g^{\mu\nu}-v^\mu v^\nu)}{2(v\cdot k-\frac{1}{4}\Delta)}$

π_{ba}

P_b $\qquad\qquad$ P^*_a $\qquad\qquad$ $= \frac{2M_P}{f_\pi}g(q\cdot\epsilon^*_b)(\pi^i\lambda^i)_{ba}$

π_{ba}

P^*_b $\qquad\qquad$ P^*_a $\qquad\qquad$ $= -\frac{2M_P}{f_\pi}g(\pi^i\lambda^i)_{ba}\epsilon_{\mu\nu\alpha\beta}\epsilon^{*\mu}_a\epsilon^\nu_b q^\alpha v^\beta$

Figure 2.3.1: Feynman rules obtained in HMχPT

Bringing all these aspects together, we can simply derive the Feynman rules for the various interactions as shown in the Feynman diagrams of Fig. 2.3.1.

CHAPTER 3

LEPTONIC B MESON DECAY AND SOFT PHOTONS

3.1 Faking $B_s \to \mu^+ \mu^-$

The rare leptonic decay of the B_s^0 into a dimuon pair, $B_s^0 \to \mu^+ \mu^-$, is an example of a flavor-changing neutral current process. Studies of such decay processes not only play an important role in determining electroweak and strong interaction parameters of the standard model of particle physics, but also serve as sensitive probes of possible physics beyond the standard model [31]. While recent evidence for observation of $B_s^0 \to \mu^+ \mu^-$ from LHC-b collaboration [32] , as well as an earlier result from CDF [33] preclude any spectacular new physics (NP) effect, there is still room for NP to influence this decay. It is then important to have a firm evaluation of $\mathcal{B}(B_s^0 \to \mu^+ \mu^-)$ in the SM [34, 35] and a firm understanding that experimentally-observed branching ratio

$$
\begin{aligned}
\mathcal{B}_{LHCb}(B_s^0 \to \mu^+ \mu^-) &= (3.2^{+1.5}_{-1.2}) \times 10^{-9} \\
\mathcal{B}_{CDF}(B_s^0 \to \mu^+ \mu^-) &= (1.8^{+1.1}_{-0.9}) \times 10^{-8}
\end{aligned}
\tag{3.1}
$$

actually corresponds to the $B_s^0 \to \mu^+ \mu^-$ transition.

As explained in Chapter 1, the $B_s^0 \to \mu^+ \mu^-$ decay is helicity suppressed in the SM by $m_\mu^2 / m_{B_s}^2$ due to the left handed nature of weak interactions [36]. This effect arises from the necessary spin flip on the outgoing back-to-back lepton pair in order to conserve angular momentum since the initial state meson is spinless.

This suppression is absent in B_s^0 decays where the muon pair is produced with one or more additional particles in the final state that can carry away a unit of angular momentum,

such as $B_s^0 \to \mu^+\mu^-\gamma$ or $B_s^0 \to \mu^+\mu^-\nu_\mu\bar\nu_\mu$. This means that, in general, those processes could have sizable total branching ratios, comparable to that of $B_s^0 \to \mu^+\mu^-$, despite being suppressed by other small parameters (such as α_{EM} for $B_s^0 \to \mu^+\mu^-\gamma$) [37]. If, in addition, the final state photon or $\nu\bar\nu$ is undetected, while the invariant mass of $\mu^+\mu^-$ pair is close to $m_{B_s^0}$, then the experimentally-measured branching ratio would correspond to

$$\mathcal{B}_{exp}(B_s^0 \to \mu^+\mu^-) = \mathcal{B}(B_s^0 \to \mu^+\mu^-) \left[1 + \sum_X \frac{\mathcal{B}(B_s^0 \to \mu^+\mu^-X)|_{m(\mu^+\mu^-)\approx m_{B_s}}}{\mathcal{B}(B_s^0 \to \mu^+\mu^-)} \right], \quad (3.2)$$

where X is an undetected particle or a group of particles. The contribution of $B_s^0 \to \mu^+\mu^-X$ would depend on how well X could be detected in a particular experiment, as well as on whether $B_s^0 \to \mu^+\mu^-X$ has any kind of resonance enhancement that is not well modeled by background models chosen by a particular experiment in a given window of $m(\mu^+\mu^-)$, as well as the size of that window. For example, for $X = \gamma$, most current searches use di-lepton energy cuts that would correspond to an allowable soft photon of up to 60 MeV. For $B \to \ell\nu_\ell$ transition and $X = \gamma$ similar effects were discussed in [38, 39, 40], and for X being light particles – in [41]. In the following we shall concentrate on the amplitudes that are non-vanishing in the $m_\mu \to 0$ limit.

3.2 $B_s^0 \to \mu^+\mu^-\gamma$ transition

Due to higher backgrounds in hadron collider experiments soft photons emitted in $B_s^0 \to \ell^+\ell^-\gamma$ could be hard to detect, so this background could be quite important. This decays were previously analyzed in [37], where a form-factor model-dependent calculation was performed [42]. The analysis presented in [37] was mainly geared towards kinematical regimes where the photon is sufficiently hard to be detected; in fact, low-energy cut-offs were introduced on photon energies. We apply a model-independent approach that incorporates

both heavy quark symmetry for hadrons containing a heavy quark with mass $m_Q \gg \Lambda_{QCD}$, and chiral $SU(3)_L \times SU(3)_R$ symmetries in the $m_q \to 0$ limit [43, 44]. We organize our calculations in terms of an expansion in $1/m_b$ and examine the contribution of terms up to leading order in $\mathcal{O}(1/m_b)$.

Similarly to $B \to \ell \nu_\ell \gamma$ [39], the decay amplitude for $B_s \to \mu^+ \mu^- \gamma$ transition can be broken into two generic parts containing internal bremsstrahlung (IB) and structure dependent (SD) contributions. The bremsstrahlung contributions are still helicity suppressed, while the SD contribution contain the electromagnetic coupling α but are not suppressed by the lepton mass. Phenomenologically, the origin of that can be understood as follows. When the soft photon in emitted from the B_s meson, heavy intermediate states including the $J^P = 1^-$ B_s^* vector meson state become possible. This lifts helicity suppression since the lepton pair couples directly to the spin 1 meson. In the kinematic regime where the photon is soft, we expect that the significant contribution comes only from the vector B_s^* resonance for reasons analogous to the B^* pole dominance in $B \to \pi \ell \nu$ at near zero pionic recoil energies [45]. This is because in the large m_b limit the B_s^* and B_s become degenerate and the residual mass splitting is $m_{B^*} - m_B \sim \mathcal{O}(1/m_b)$ [46]. Therefore the excitation of the B_s^* does not require much energy. There are two diagrams containing an intermediate B_s^* as seen in Fig. 3.2.1. In the kinematic region of interest where $E_\gamma < 60 MeV$, Fig. 3.2.1 (b) where the intermediate B_s^* decays to an on-shell soft photon is $(1/M_{B_s^0})$ suppressed and will be neglected. Similarly, a contribution of Fig. 3.2.1 (c) is formally $(1/M_{B_s^0})$, so it will be neglected in what follows.

The calculation of soft photon effects should carefully deal with soft divergencies. Those are cancelled between one-loop radiative corrections to $B_s \to \mu^+ \mu^-$ and $B_s \to \mu^+ \mu^- \gamma$.

We employ heavy meson chiral perturbation theory (HMχPT) to calculate the amplitude for Fig. 3.2.1 (a). The heavy meson superfield H_a contains both the B_s^0 and B_s^{*0} bosons,

$$H_a = \frac{1 + \not{v}}{2}(B_{a\mu}^* \gamma^\mu - B_a \gamma_5), \qquad \bar{H}_a = \gamma^0 (H_a)^\dagger \gamma^0, \qquad (3.3)$$
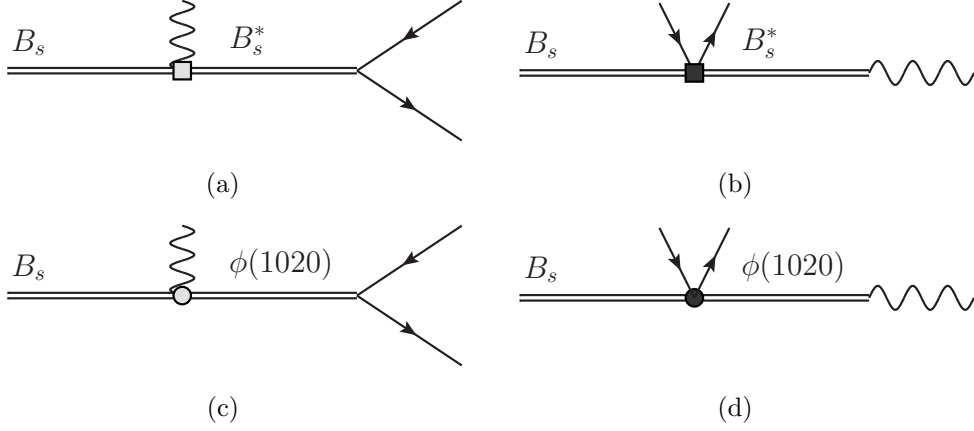
Figure 3.2.1: Resonant contributions to $B_s \to \mu^+\mu^-\gamma$

where the indices a and b reflect the light quark flavor indices. The light mesons are introduced through the matrix $Q^\xi = \frac{1}{2}(\xi^\dagger Q\xi + \xi Q\xi^\dagger)$ where the field $\xi = \exp(i\Pi/f)$ is defined in terms of a 3×3 unitary matrix containing the octet of pseudo-Goldstone bosons

$$\Pi = \begin{pmatrix} \frac{\pi^0}{\sqrt{2}} + \frac{\eta}{\sqrt{6}} & \pi^+ & K^+ \\ \pi^- & -\frac{\pi^0}{\sqrt{2}} + \frac{\eta}{\sqrt{6}} & K^0 \\ K^- & \bar{K}^0 & -\sqrt{\frac{2}{3}}\eta \end{pmatrix}. \tag{3.4}$$

To evaluate diagram Fig. 3.2.1 (a) we need an amplitude for a $B \to B^*\gamma$ transition as

$$\mathcal{M}_{[B_s \to B_s^*\gamma_s \to \mu^+\mu^-\gamma_s]} = \mathcal{M}^\mu_{B_s^* \to \mu^+\mu^-} \times \frac{g_{\mu\alpha}}{M_{B_s^*}^2} \times \mathcal{M}^\alpha_{B_s \to B_s^*\gamma}, \tag{3.5}$$

The amplitude for $B \to B^*\gamma$ is conventionally parameterized as

$$\mathcal{M}_{B_s \to B_s^*\gamma} = -ie\mu\eta_\alpha^* v_\beta k_\mu \epsilon_\nu^* \epsilon^{\mu\nu\alpha\beta}, \tag{3.6}$$

where k is the 4-momentum of the photon, v the velocity of the decaying heavy meson, η is the vector meson polarization, and ϵ is the photon polarization. The strength of the transition is
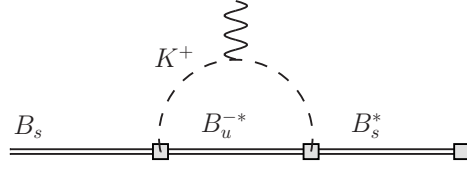
Figure 3.2.2: One loop corrections to μ. The double lines denote the heavy mesons B and B^* while the single line denotes the goldstone bosons

described by the magnetic moment, μ, which receives contributions from the photon coupling to both heavy and the light quark components of the electromagnetic current [47],

$$\mu = \mu_b + \mu_\ell. \tag{3.7}$$

The bottom quark contribution is fixed by heavy quark symmetry to be $\mu_b = Q_b/m_b = -1/(3m_b)$, while the light quark contribution can be computed, to one loop, in HMχPT. The relevant effective Lagrangian is [47, 48]

$$\mathcal{L}_\beta = \frac{\beta e}{4} \text{Tr}(\bar{H}_a H_b \sigma^{\mu\nu} F_{\mu\nu} Q_{ba}^\xi) + \frac{ig}{2} \text{Tr} \left(\bar{H}_a H_b \gamma_\mu \gamma_5 (\xi^\dagger \partial^\mu \xi - \xi \partial^\mu \xi^\dagger)_{ba} \right), \tag{3.8}$$

where Tr is a trace over the Dirac indices, and β is a coupling constant parameterizing a local contribution to the light quark magnetic moment. We include the most important one-loop correction, which is shown in Fig. 3.2.2.

The effective magnetic moment for the $B_s \to B_s^* \gamma$ transition is then

$$\mu_{B_s\gamma} = -\frac{1}{3m_b} - \frac{1}{3}\beta + g^2 \frac{m_K}{4\pi f_K^2}, \tag{3.9}$$

where g is the χPT coupling constant, and m_K, f_K are the mass and decay constant of the kaon respectively. The constants β and g can be extracted from a combination of the experimental D^{*+} branching ratios, $\mathcal{B}(D^{*+} \to D^+\gamma) = 0.016 \pm 0.004$ and $\mathcal{B}(D^{*+} \to D^0\pi^+) = 0.677 \pm 0.005$, and the total width, where the newest preliminary result from

BaBar collaboration is reported to be $\Gamma_{D^{*+}} = 83.5 \pm 1.7 \pm 1.2$ KeV [49]. The decay widths for these processes using the method above are given by

$$\Gamma(D^{*+} \to D^+\gamma) \;\; = \;\; \frac{\alpha_{EM}}{3}\left(\frac{2}{3m_c} - \frac{1}{3}\beta + g^2\frac{m_\pi}{4\pi f_\pi^2}\right)^2 |\vec{k}|^3, \tag{3.10}$$

$$\Gamma(D^{*+} \to D^0\pi^+) \;\; = \;\; \frac{g^2}{6\pi f_\pi^2}|\vec{p_\pi}|^3. \tag{3.11}$$

This yeilds the approximate values of the coupling constants, $g \approx 0.552$ and $\beta \approx 7.29 GeV^{-1}$. With Eq.3.9 this gives us $|\mu_{eff}| \approx 1.13$ GeV^{-1}.

To complete evaluation of Fig. 3.2.1 (a) in Eq. (3.5), we evaluate the $B_s^* \to \mu^+\mu^-$ transition. The effective hamiltonian describing the weak $b \to s\ell^+\ell^-$ transition is

$$\mathcal{H}_{b \to s\bar{\ell}\ell} = \frac{G_F}{\sqrt{2}}V_{tb}V_{ts}^*\frac{e^2}{8\pi^2}\left[\bar{s}\gamma^\mu(1 \;\; - \;\; \gamma_5)b \cdot \bar{\ell}\left[C_{9V}^{eff}(\mu, q^2)\gamma_\mu + C_{10A}(\mu^2)\gamma_\mu\gamma_5\right]\ell\right.$$
$$\left. - \;\; 2im_b\frac{C_{7\gamma}(\mu^2)}{q^2}q_\nu \cdot \bar{s}\sigma^{\mu\nu}(1 + \gamma_5)b \cdot \bar{\ell}\gamma_\mu\ell\right], \tag{3.12}$$

where $q_\nu = (p_{\ell^+} + p_{\ell^-})_\nu$ is the momentum of the lepton pair and C_i are scale-dependent Wilson coefficients. The matrix element for $B_s^* \to \mu\bar{\mu}$ is then

$$\mathcal{M}_{B_s^* \to \mu^+\mu^-} \;\; = \;\; i\frac{G_F}{\sqrt{2}}V_{tb}V_{ts}^*\frac{e^2}{8\pi^2}f_{B_s}M_{B_s}\left[\eta_\mu^*\bar{u}(p_{\mu^+})[C_9\gamma^\mu + C_{10}\gamma^\mu\gamma_5]v(p_{\mu^-})\right.$$
$$\left. - \;\; 2m_b\frac{C_7}{q^2}(\bar{u}(p_{\mu^+})\gamma_\mu v(p_{\mu^-}))q_\nu(i\epsilon^{\mu\nu\alpha\beta}v_\alpha\eta_\beta + v^\mu\eta^\nu - v^\nu\eta^\mu)\right], \tag{3.13}$$

where η^μ and v^μ are the polarization and 4-velocity of the vector meson respectively. We defined $\langle 0|\bar{s}_L\gamma^\mu b_L|B_s^*\rangle = \eta^\mu f_{B_s^*}/2$, and $\langle 0|\bar{s}\sigma^{\mu\nu}(1 + \gamma_5)b|B_s^*\rangle = M_B f_{B_s}[i\epsilon^{\mu\nu\alpha\beta}v_\alpha\eta_\beta + v^\mu\eta^\nu - v^\nu\eta^\mu]$, with $f_{B_s^*} = M_{B_s}f_{B_s}$ [50]. This gives for the amplitude of Fig. 3.2.1 (a)

$$\mathcal{M}_{[B_s \to B_s^*\gamma_s \to \mu^+\mu^-\gamma_s]} \;\; = \;\; \frac{G_F}{\sqrt{2}}V_{tb}V_{ts}^*\frac{e^3}{8\pi^2}\mu_{eff}\frac{f_{B_s}}{q^2 - M_{B_s^*}^2}\left(\epsilon^{\mu\nu\alpha\beta}\epsilon_\mu^* k_\alpha q_\beta\right)$$
$$\times \;\; \left[\left(2C_7m_b - C_9M_{B_s^*}\right)\left[\bar{u}_{p_1}\gamma_\nu v_{p_2}\right] - C_{10}M_{B_s^*}\left[\bar{u}_{p_1}\gamma_\nu\gamma_5 v_{p_2}\right]\right]. \tag{3.14}$$

The other contribution that is leading the $M_{B_s} \to \infty$ limit is given in Fig. 3.2.1 (d)

$$\mathcal{M}_{[B_s^0 \to \mu\bar{\mu}\phi \to \mu\bar{\mu}\gamma_s]} = \mathcal{M}_{B_s^0 \to \mu\bar{\mu}\phi} \times \frac{g_{\mu\nu}}{m_\phi^2} \times \mathcal{M}_{\phi \to \gamma_s}, \tag{3.15}$$

Employing vector-meson dominance, and using the definition of the vector meson decay constant $\langle 0|\bar{s}\gamma^\mu s|\phi\rangle = f_\phi m_\phi \eta_\phi^\mu$, where η_ϕ^μ is the polarization of the ϕ meson, and $\langle\gamma|\bar{s}(-ieQ_s \ / \ A)s|\phi\rangle = (-ieQ_s)\epsilon_\mu^*\langle 0|\bar{s}\gamma^\mu s|\phi\rangle$,

$$\mathcal{M}_{\phi \to \gamma_s}^\mu = \frac{1}{3} e f_\phi m_\phi \epsilon_\mu^*. \tag{3.16}$$

Again, we calculate $\mathcal{M}_{B_s^0 \to \mu\bar{\mu}\phi}$ using (HMχpT). For the short distance contributions we use the effective Hamiltonian describing $b \to s\ell\ell$ transitions in Eq. 3.12, as well as the effective Hamiltonian for $b \to s\gamma$,

$$\mathcal{H}_{b \to s\gamma} = \frac{G_F}{\sqrt{2}} V_{tb} V_{ts}^* \frac{e}{8\pi^2} m_b C_{7\gamma}(\mu^2) \cdot \bar{s}\sigma^{\mu\nu}(1+\gamma_5)b \cdot F_{\mu\nu}. \tag{3.17}$$

In order to bosonize the quark currents found in Eqs. (3.12) and (3.17) we introduce the light vector octet to the HMχpT [50],

$$\rho_\mu \equiv i\frac{g_V}{\sqrt{2}} \begin{pmatrix} \frac{\rho^0}{\sqrt{2}} + \frac{\omega}{\sqrt{2}} & \rho^+ & K^{*+} \\ \rho^- & -\frac{\rho^0}{\sqrt{2}} + \frac{\omega}{\sqrt{2}} & K^{*0} \\ K^{*-} & \bar{K}^{*0} & \phi \end{pmatrix}. \tag{3.18}$$

The bosonized currents $\bar{s}\gamma^\mu(1-\gamma_5)b$ and $\bar{s}\sigma^{\mu\nu}(1+\gamma_5)b$ are, respectively,

$$\begin{aligned} L_{1a}^\mu &= \alpha_1 \langle \gamma_5 H_b (\rho^\mu)_{bc} \xi_{ca}^\dagger \rangle, \\ L_{1a}^{\mu\nu} &= i\alpha_1 \left\{ g^{\mu\alpha} g^{\nu\beta} - \frac{i}{2}\epsilon^{\mu\nu\alpha\beta} \right\} \langle \gamma_5 H_b [\gamma_\alpha(\rho_\beta)_{bc} - \gamma_\beta(\rho_\alpha)_{bc}]\xi_{ca}^\dagger \rangle. \end{aligned} \tag{3.19}$$

A numerical value of $\alpha_1 = -0.07 \, GeV^{1/2}$ [50] will be used for our calculations. Keeping only the gauge invariant portion, the amplitude for the decay with an intermediate $\phi(1020)$ is

$$
\begin{aligned}
\mathcal{A}(B_s^0 \to \mu\bar{\mu}\phi \to \mu\bar{\mu}\gamma_s) \;=\; & G_F V_{tb} V_{ts}^* \frac{e^3 f_\phi g_\phi \alpha_1 C_7 m_b}{24\pi^2 \sqrt{M_{B_s}} m_\phi(p_1 \cdot p_2)} \epsilon_\mu^* \bigg((k \cdot (p_1 + p_2))[\bar{u}_{p_1} \gamma^\mu v_{p_2}] \\
& - (p_1 + p_2)^\mu[\bar{u}_{p_1} \slashed{k} v_{p_2}] + i\epsilon^{\mu\nu\alpha\beta} k_\alpha (p_1 + p_2)_\beta [\bar{u}_{p_1} \gamma_\nu v_{p_2}] \bigg). \quad (3.20)
\end{aligned}
$$

We checked that other contributions to the decay are smaller then the ones considered above. We considered the bremsstrahlung diagrams where a soft photon is emitted from one of the outgoing leptons. These diagrams will result in an infrared divergence in the soft region, which has been shown to cancel with the 1-loop QED vertex corrections [51]. The vertex corrections, as well as the bremsstrahlung contributions, will remain suppressed by a power of the lepton mass. Therefore the remaining non-divergent contributions from both the bremsstrahlung and vertex corrections to final states with either an electron or a muon would not be significant.

The only contribution to the ampltitude from the effective hamiltonian describing the weak transition in Eq.(3.12) ends up being the $\mathcal{O}_{10}$ operator. This come from obtaining the matrix elements for the pseudoscalar meson,

$$
\langle 0|(\bar{s}\gamma^\mu(1 - \gamma_5)b)|B_s\rangle \;=\; -if_B P_B^\mu, \qquad (3.21)
$$

$$
\langle 0|(\bar{s}\sigma^{\mu\nu}(1 + \gamma_5)b)|B_s\rangle \;=\; 0, \qquad (3.22)
$$

where f_B is the decay constant of the B meson. With these definitions and using the conservation of the vector current we can arrive at an expression for the amplitude

$$
\mathcal{M}_{Brem} = ie \frac{\alpha_{EM} G_F}{2\sqrt{2}} V_{tb} V_{ts}^* f_B C_{10} m_\mu \left[\bar{\mu} \left(\frac{\slashed{\epsilon} \slashed{P}_B}{p_{\mu^-} \cdot k} - \frac{\slashed{P}_B \slashed{\epsilon}}{p_{\mu^+} \cdot k} \right) \gamma_5 \mu \right], \qquad (3.23)
$$

where ϵ^μ and k are the polarization and momentum of the photon respectively. Just as

we would expect from the helicity structure involved, the amplitude for the bremsstrahlung contribution is proportional to the lepton mass. So in the limit $m_\ell \to 0$, this contribution should be negligible compared to the non helicity-suppressed contributions.

Putting everything together, the distribution of the decay width as a function of the kinematic variable $s = (P_{B_s} - k)^2/M_{B_s}^2 = q^2/M_{B_s}^2$, in the limit $m_\ell \to 0$,

$$\frac{d\Gamma}{ds} = \frac{d\Gamma}{ds}\bigg|_{B_s^*} + \frac{d\Gamma}{ds}\bigg|_{\phi B_s^*} + \frac{d\Gamma}{ds}\bigg|_{\phi}, \tag{3.24}$$

where the decay distributions are given for the two different resonance amplitudes and their interference.

$$\frac{d\Gamma}{ds}\bigg|_{B_s^*} = X_{CKM} M_{B_s}^3 f_{B_s}^2 \mu_{eff}^2 \left[(|C_9|^2 + |C_{10}|^2)x_{B^*} + 4\,C_7^2 x_b - 4\,C_7 C_9 x_b x_{B^*}\right] \frac{s(1-s)^3}{(s - x_{B_s^*}^2)^2},$$

$$\frac{d\Gamma}{ds}\bigg|_{\phi} = X_{CKM} \left[\frac{16\,C_7^2\,f_\phi^2\,g_\phi^2\,m_b^2\,\alpha_1^2}{9\,m_\phi^2}\right] \frac{(1-s)^3}{s}, \tag{3.25}$$

$$\frac{d\Gamma}{ds}\bigg|_{\phi B_s^*} = X_{CKM} \left[\frac{4\sqrt{2}f_{B_s}f_\phi g_\phi M_{B_s}^{3/2} m_b \alpha_1 \mu_{eff}}{3m_\phi}(C_7 C_9 x_{B^*} - 2C_7^2 x_b)\right] \frac{(1-s)^3}{s - x_{B_s^*}^2},$$

where we have defined $X_{CKM} = (G_F^2|V_{tb}V_{ts}^*|^2 M_{B_s}^2 \alpha_{EM}^3)/(768\pi^4)$, $x_b \equiv m_b/M_{B_s}$, and $x_{B_s^*} \equiv M_{B_s^*}/M_{B_s}$. We use the Wilson coefficients $C_i(\lambda)$ choosing the scale at $\lambda \simeq m_b \simeq 5 GeV$, with $C_7 = 0.312$, $C_9 = -4.21$ and $C_{10} = 4.64$ [37][52]. The CKM matrix elements are $|V_{tb}V_{ts}^*| = (4.7 \pm 0.8) \times 10^{-2}$ [53]. With the most recent lattice calculation of f_{B_s} is ≈ 228 MeV [54]. Note that, when integrated over the endpoint window the last two terms in Eq. (3.24) are much smaller than the first one. The interference contribution is destructive and is

$$\mathcal{B}(B_s \to \mu^+\mu^-\gamma_{E<60})_{\phi B_s^*} = -5.0 \times 10^{-17}, \tag{3.26}$$

$$\mathcal{B}(B_s \to \mu^+\mu^-\gamma_{E<300})_{\phi B_s^*} = -1.1 \times 10^{-14}, \tag{3.27}$$
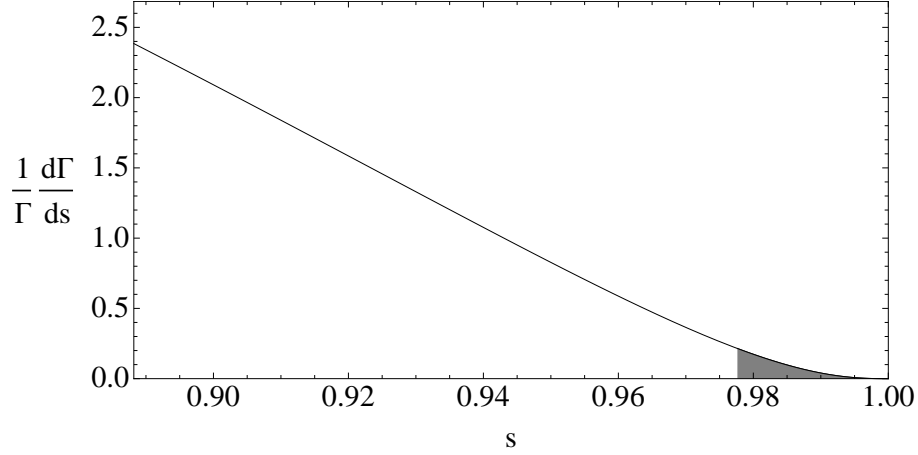
Figure 3.2.3: Normalized differential spectrum in s. The grey shaded region corresponds to the contribution from a soft photon energy cut at $E_\gamma \sim 60$ MeV.

which are both much smaller than the B_s^* contribution alone.

The normalized differential spectrum in s is shown in Fig.(3.2.3). The photon energy is related to the invariant mass as $E_\gamma = (1 - s)M_B/2$, so we can integrate the differential spectrum over the required corresponding kinematic region in photon energy to obtain the decay width.

Integrating Eq.(3.24) over the kinematic region corresponding to a soft photon cut of $E_\gamma \sim 60, 300$ MeV we get the respective branching ratios

$$\mathcal{B}(B_s \to \mu^+\mu^-\gamma_{E<60}) = 1.6 \times 10^{-12}, \tag{3.28}$$

$$\mathcal{B}(B_s \to \mu^+\mu^-\gamma_{E<300}) = 1.1 \times 10^{-10}, \tag{3.29}$$

which are quite too low to affect experimental determination of the branching ratio $B_s \to \mu^+\mu^-$, agreeing with the estimates of Ref. [34] where $\mathcal{B}_{\mathcal{SM}}(B_s^0 \to \mu^+\mu^-) = (3.23 \pm 0.27) \times 10^{-9}$.
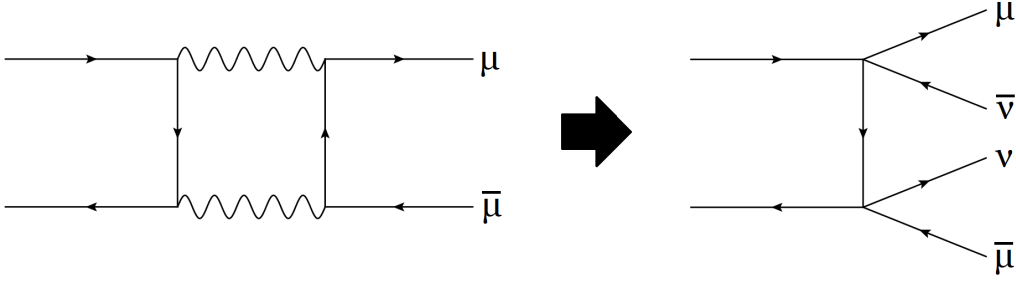
Figure 3.3.1: $B_s \to \mu^+ \mu^- \bar{\nu} \nu$

3.3 $B_s^0 \to \mu^+ \mu^- \nu_\mu \bar{\nu}_\mu$ transition

Because of the Glashow-Illiopulous-Maiani (GIM) mechanism, the SM loop diagram for the helicity-suppressed $B_s^0 \to \mu^+ \mu^-$ decay is dominated by the intermediate top quark despite being suppressed by the CKM factors $|V_{tb} V_{ts}^*|^2$. A transition similar to the ones described above, which on a portion of the available phase space looks like $B_s^0 \to \mu^+ \mu^-$ is the tree-level decay $B_s^0 \to \mu^+ \mu^- \nu \bar{\nu}$. The dominant tree-level contribution for this process is depicted in Fig. 3.3.1. This decay can have a contribution to the background, which appears only below $q^2 = M_{B_s}^2$ and, if numerically significant, can affect the extraction of $\mathcal{B}(B_s \to \mu^+ \mu^-)$. This process is neither loop-dominated nor is it helicity suppressed. It nevertheless has a kinematic phase space suppression due to the four-particle final state. For the B_s meson decay, an intermediate charm quark will give the largest contribution since the intermediate top quark diagram will be suppressed by the mass of the top quark. Also, the up quark contribution is suppressed by $V_{ub} V_{us}^* \approx \lambda^4$ whereas the charm contribution is only suppressed by $V_{cb} V_{cs}^* \approx \lambda^2$, where $\lambda \approx 0.22$.

The transition amplitude for this process is simple,

$$\mathcal{M}_{B_s \to \mu^+ \mu^- \nu \bar{\nu}} = \frac{G_F^2}{2} V_{cb} V_{cs}^* \langle 0 | \bar{s} \gamma_\beta (1 - \gamma_5) \frac{i(\not{p}_c + m_c)}{p_c^2 - m_c^2} \gamma_\alpha (1 - \gamma_5) b | B_s \rangle L_1^\alpha L_2^\beta, \tag{3.30}$$

where $L^\alpha = \bar{\mu}\gamma^\alpha(1-\gamma_5)\nu_\mu$. In the rest frame of the decaying meson we can reduce the phase space integral's dependence to five independent Lorentz invariants. In the same fashion as in [55] we define these invariants as

$$S_{12} = (p_{\mu^-} + p_{\mu^+})^2, \quad S_{13} = (p_{\mu^-} + p_{\bar{\nu}})^2, \quad S_{34} = (p_{\bar{\nu}} + p_\nu)^2,$$

$$S_{123} = (p_{\mu^-} + p_{\mu^+} + p_{\bar{\nu}})^2 \quad , \quad S_{134} = (p_{\mu^-} + p_{\bar{\nu}} + p_\nu)^2. \tag{3.31}$$

Our width then becomes

$$d\Gamma = \frac{(2\pi)^4}{2M} \int \left(\frac{\pi^2}{2M^2}\right) \frac{|\mathcal{M}_{B_s\to\mu^+\mu^-\nu\bar{\nu}}|^2}{[-\Delta_4(p_{\mu^-}, p_{\mu^+}, p_{\bar{\nu}}, p_\nu)]^{1/2}} dS_{12} dS_{123} dS_{13} dS_{134}, \tag{3.32}$$

where Δ_4 is the symmetric Gram determinant

$$\Delta_4(q, r, s, t) = \begin{vmatrix} q^2 & q \cdot r & q \cdot s & q \cdot t \\ r \cdot q & r^2 & r \cdot s & r \cdot t \\ s \cdot q & s \cdot r & s^2 & s \cdot t \\ t \cdot q & t \cdot r & t \cdot s & t^2 \end{vmatrix}. \tag{3.33}$$

In order to avoid the divergence of $1/(-\Delta_4)^{1/2}$ on the boundary, suitable variable changes can be made thereby making the singularity integrable. We define

$$S_{134} = \frac{1}{2a}\left[-b + \sin(\tilde{S}_{134})(b^2 - 4ac)^{1/2}\right],$$

$$S_{13} = 4(-a)^{1/2}\tilde{S}_{13} + m_\ell^2, \tag{3.34}$$

where a, b and c are the parameters solved by

$$-\Delta_4(p_{\mu^-}, p_{\mu^+}, p_{\bar{\nu}}, p_\nu) = aS_{134}^2 + bS_{134} + c. \tag{3.35}$$

The limits of integration are calculated in [55], resulting in our partial width

$$\frac{d\Gamma}{dS_{12}} = \frac{2}{(4\pi)^6 M^3} \int_{S_{12}}^{M^2} dS_{123} \int_0^\xi dS_{34} \int_{m_\ell^2/S_{12}}^1 d\tilde{S}_{13} \int_{-\pi/2}^{\pi/2} d\tilde{S}_{134} \left| \mathcal{M}_{B_s \to \mu^+\mu^-\nu\bar{\nu}} \right|^2, \quad (3.36)$$

where $\xi = (M^2 - S_{123})(S_{123} - S_{12})/S_{123}$. We define the cut on missing energy as $S_{12}^{cut}(E_{cut}) = M^2 - 2M(E_{cut})$ which gives us a lower limit on S_{12} for the final integral in order to obtain the decay width. The branching ratios for this contribution can then calculated using numerical phase-space integration for various cuts including the one that corresponds to the invariant mass range seen at the LHCb [32].

$$\mathcal{B}\left[B_s \to \mu^+\mu^-\nu\bar{\nu}\right]_{E_{cut}=60MeV} = 1.6 \times 10^{-25}$$
$$\mathcal{B}\left[B_s \to \mu^+\mu^-\nu\bar{\nu}\right]_{E_{cut}=300MeV} = 1.4 \times 10^{-18}. \quad (3.37)$$

As we can see, the due to enormous phase space suppression (we are only interested in a small sliver of the available four-particle final state), the possible contribution from this decay is unimportant for experimental analyses.

3.4   Results

Recent evidence from observation of the flavor-changing neutral current decay $B_s^0 \to \mu^+\mu^-$ by the LHCb collaboration $\mathcal{B}(B_s^0 \to \mu^+\mu^-) = (3.2_{-1.2}^{+1.5}) \times 10^{-9}$ is consistent with the latest standard model predictions. We analyzed branching ratios of the decays $B_s^0 \to \mu^+\mu^-X$, with $X = \gamma$ or $\nu\bar{\nu}$, which can mimic $B_s^0 \to \mu^+\mu^-$ on portions of the parameter space where X is soft. We performed a model-independent calculation of those processes incorporating heavy quark and chiral symmetries of QCD. Our calculations concentrated on the contributions that are not helicity suppressed by powers of m_μ and leads to a correction

to the SM prediction of approximately 3% at a photon energy cut of 300 MeV and less than 1% at a cut of 60 MeV from soft photon contributions to the decay $B_s \to \mu^+ \mu^-$. The possible contamination from $B_s \to \mu^+ \mu^- \nu \bar{\nu}$ is even smaller, at the sub percent level.

CHAPTER 4

EXCLUSIVE W DECAY IN EFFECTIVE FIELD THEORY

4.1 General Analysis of $W \to P + \gamma$ and its motivation

We begin by taking a look at the radiative exclusive decay mode of the W boson, focusing on $W^\pm \to \pi^\pm + \gamma$. The W, which is a massive charged vector boson that mediates weak interactions can decay into the a light pseudoscalar meson such as the pion which is the bound state of an up and down quark (or charm and strange quarks in the case of a $D_s^\pm$ meson), and a real photon which is massless but energetic.

Intermediate vector bosons like the W are produced in high energy accelerators and the study of such exclusive decay modes would provide very useful insight into electroweak and strong interaction dynamics. High luminosity colliding beam facilities of pp, $\bar{p}p$, or e^+e^- collisions can produce Intermediate W bosons copiously and precise measurements of their basic properties can then be analyzed [56]. In order to do this we need to learn as much as possible about the theoretically predicted decay modes of these particles and pin down their decay rates in the standard model. Although the decay modes discussed in this chapter are rare, we can expect that these radiative decays could be observable in the future with increased statistics at high luminosity colliders. Prospectively then, getting a good grip on the standard model analysis can inform us about the room for discovery of new physics or exotic particles and mesons in the decay products of intermediate vector bosons [57]. There is also interest in measurements of W boson decay to pseudoscalar and vector particles at experiments like the Tevatron and LHC [58]. The current experimental bound [59] from the CDF at the Tevatron for the radiative W decay to a pion and a photon in $p\bar{p}$ collisions is

$$\mathcal{B}r_{EXP}[W^\pm \to \pi^\pm\gamma] < 8 \times 10^{-5}. \tag{4.1}$$

$$\pi^{-} \longleftarrow \quad \widehat{W^{-}} \sim\!\sim\!\sim\!\sim\!\sim\!\sim \quad \gamma$$

Figure 4.1.1: Two body decay of W in its rest frame

So we can see there is much room for theoretical analysis and improvement. Experimentally the $W \to \pi\gamma$ channel is interesting since it results in a clean final state in the detector. If observed these exclusive decays would yield insight into the strong interaction effects involved in the formation of the meson. Furthermore, the trilinear non-Abelian gauge coupling that appears in these decays [Fig.4.2.1(a)] according to the standard model for weak interactions can also be tested. Therefore these processes could be sensitive to physics beyond the standard model involving anomalous coupling of the photon to the W boson.

The W boson is predicted to have a mass by the standard $SU(2)_L \times U(1)$ Weinberg-Salam model for weak interactions. The Particle Data Group (PDG) combine the measurements from the LEP and Tevatron experiments to give a world average for the W mass [60, 61]

$$M_W = 80.385 \pm 0.015 \quad GeV. \tag{4.2}$$

Detection of its radiative decay along with the measurement of the photon energy can be used to obtain an extremely precise determination of this mass provided the decay rate is large enough. So a good theoretical calculation of these rare decay modes is significant and can provide an important precision test of the standard model.

One can see this by noticing the kinematics that is dictated by this two-body decay. In the rest frame of the initially decaying W boson the final products of the decay will have momentum in opposite directions as shown in Fig.4.1.1. The photon that is produced is real, and being massless it is highly energetic. Therefore the pion, which is light in mass, is kicked in the opposite direction with an energy of about half the center of mass energy provided by the W mass. Therefore the quarks that are bound in the pion are collinear and

any transverse components essentially become negligible. We can neglect the mass of the pion since it is quite smaller than the hard scale Q defined in this problem by the mass of the decaying W boson so that $m_\pi < Q \sim m_W$.

There have been previous studies of $W \to P\gamma$, where P is a pseudo scalar meson (π, D_s) using particular models [62, 63]. Arnellos, Marciano and Parsa [62] assume Brodsky-Lepage form factors obtained from QCD calculation of $\pi\gamma^*\gamma$ with an off shell photon in the asymptotic limit. They obtain a branching ratio $\mathcal{B}r \sim 10^{-8}$ and suggest that a detailed QCD analysis should be carried out for the case of the axial vector form factor. On the other hand, Keum and Pham [63] obtain a substantial enhancement of about two orders of magnitude with a branching ratio $\mathcal{B}r \sim 10^{-6}$. They employ a particular quark model and use triangle diagrams with an effective yukawa type quark-pion coupling containing the constituent quark masses in order to form the meson. One of our motivations in this project is to verify the existence of this enhancement in a model independent discussion.

We estimate the branching ratio for these exclusive processes, specifically $W \to \pi + \gamma$, in the context of perturbative QCD as well as effective field theories. The mass of the W boson gives us a hard scale m_W and the only other scale is given by the collinear pion. So the dynamics and kinematics of the problem suggests that SCET would be most relevant as a playground for understanding these decays which involve the emission of an energetic photon and a meson which is a collinear bound state of the quarks. We would like to emphasize a model independent approach in our calculations. We intend to also include one-loop contributions of up to order α_s corrections and resummation of any leading logarithmic terms.

General structure of the amplitude

Even before we start calculating Feynman diagrams we can say a lot about what the amplitude for the $W \to \pi\gamma$ decay should look like. The only free Lorentz covariant parameters we

have to work with are the final state four-momenta of the photon k, and the pion P. Conservation of energy-momentum constrains the initial state W momentum to be the sum of these two. We also have the polarization vectors for the two vector bosons, $\epsilon_\mu(k)$ corresponding to the photon wavefunction and $\epsilon_\lambda(P + k)$ corresponding to the W boson wavefunction. The orthgonality conditions given by the equations of motions for the polarizations of the vector particles requires that $\epsilon(k) \cdot (k) = \epsilon(P + k) \cdot (P + k) = 0$ and also $k^2 = 0$. We must also impose the requirements of Lorentz invariance and gauge invariance. We can then obtain the general structure of the amplitude in terms of the form factors

$$\mathcal{M} = -\frac{ge}{2\sqrt{2}}|V_{ud}|[H_2(P \cdot k g^{\mu\lambda} - P_\mu k_\lambda) + iH_6 \epsilon^{\alpha\beta\mu\lambda} k_\alpha P_\beta]\epsilon_\mu^*(k)\epsilon_\lambda(P + k). \qquad (4.3)$$

H_2 is the form factor corresponding to the axial-vector component of the weak current and H_6 is the vector form factor corresponding to the electromagnetic component of the weak charged current involved. Therefore the amplitude can be reduced simply to two Lorentz structures where the form factors which are functions of the hard scale incorporate all strong interaction effects. The problem then just boils down to calculating the form factors in a convenient theory.

4.2 $W \to \pi\gamma$ in perturbative QCD

We begin with the leading order calculation of the W decay in perturbative qcd. The photon in the two body decay $W^\pm \to \pi^\pm\gamma$ is a real, hard photon and we shall calculate the amplitudes for the diagrams in the low pion mass limit where essentially $m_\pi \to 0$. There are three diagrams that contribute to the amplitude as shown in Fig. 4.2.1. The first diagram is the W pole contribution and the next two are the structure dependent diagrams with the emission of the photon from the quark legs. The initial W^- boson has a momentum $P + k$
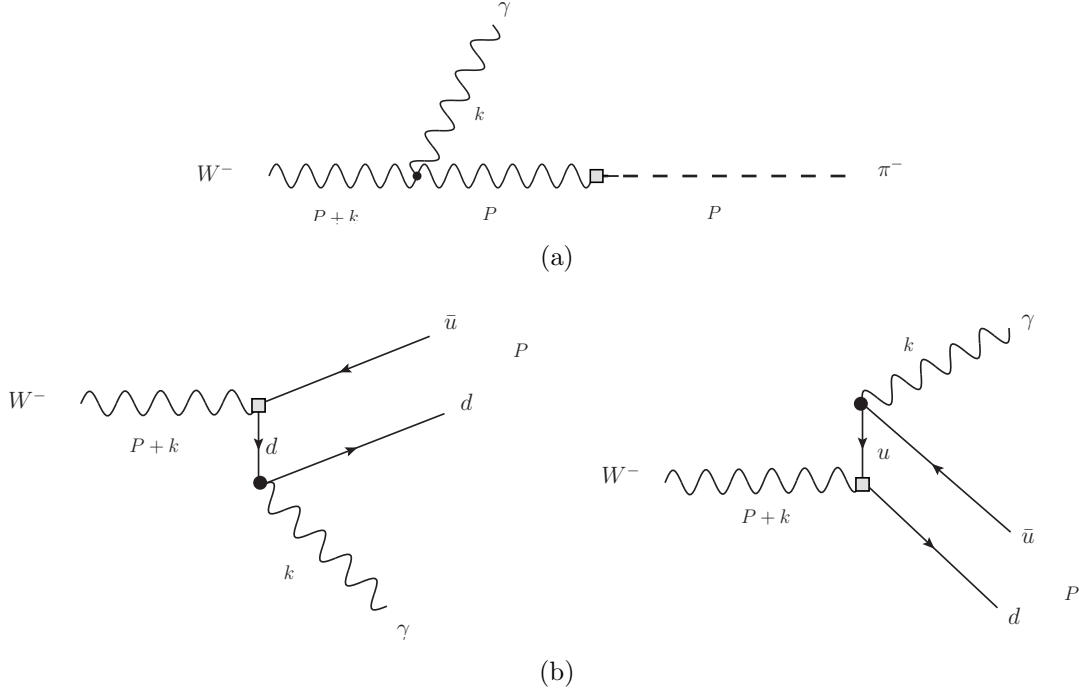
Figure 4.2.1: Tree level contributions to $W^- \to \pi^- \gamma$

which decays to a Pion with momentum P and the hard photon with momentum k. The case of the W^+ decay is obtained simply by charge conjugation.

To evaluate the first diagram we use the Weinberg Salam model for the weak couplings,

$$-ie[(2P + k)_\mu g_{\alpha\lambda} - (P + 2k)_\alpha g_{\mu\lambda} - (P - k)_\lambda g_{\mu\alpha}],$$

$$-i\frac{g}{2\sqrt{2}},$$

that are involved in the WWγ vertex and the coupling of the intermediate W to the weak charged current in the pion respectively. Including the intermediate W propagator carrying momentum P and the polarization vectors for the decaying W boson and the external photon we obtain the amplitude

$$\mathcal{M}_W = -\frac{eg}{2\sqrt{2}}|V_{ud}|f_\pi\epsilon_\mu^*(k)\epsilon_\lambda(P+k)\frac{(g^{\alpha\beta}-P^\alpha P^\beta/m_W^2)}{P^2-m_W^2}$$
$$\times[(2P)_\mu g_{\alpha\lambda}-(P+2k)_\alpha g_{\mu\lambda}-2P_\lambda g_{\mu\alpha}]P_\beta, \tag{4.4}$$

where we use the pion decay constant defined by the matrix element

$$\langle\pi|\bar{d}\gamma_\beta(1-\gamma_5)u|0\rangle = if_\pi P_\beta. \tag{4.5}$$

Using the orthogonality conditions $\epsilon_\mu(k)k_\mu = 0$ and $\epsilon_\lambda(P+k)(P+k)_\lambda = 0$, the amplitude in the massless pion limit therefore simplifies to

$$\mathcal{M}_W = -\frac{eg}{2\sqrt{2}}|V_{ud}|f_\pi\epsilon_\mu^*(k)\epsilon_\lambda(P+k)g_{\mu\lambda}, \tag{4.6}$$

so we see that this W pole diagram contributes only to the axial-vector form factor H_2.

The structure dependent amplitude can be written for the diagrams involving the emission of the photon from the quarks at tree level. We can ignore the light quark masses in the following expressions

$$\mathcal{M}_d = \frac{-ige}{2\sqrt{2}}Q_d\langle\pi|\bar{d}\gamma^\mu\frac{(\not{P}_d+\not{k})}{(P_d+k)^2}\gamma^\lambda(1-\gamma_5)u|0\rangle\epsilon_\mu^*(k)\epsilon_\lambda(P+k) \tag{4.7}$$

$$\mathcal{M}_u = \frac{-ige}{2\sqrt{2}}Q_u\langle\pi|\bar{d}\gamma^\lambda(1-\gamma_5)\frac{(-\not{P}_u-\not{k})}{(P_u+k)^2}\gamma^\mu u|0\rangle\epsilon_\mu^*(k)\epsilon_\lambda(P+k) \tag{4.8}$$

In order to describe the distribution of the quark momenta within the pion we can assign longitudinal momentum fractions to them with respect to the total outgoing pion momentum

such that

$$P_d = xP \tag{4.9}$$

$$P_u = \bar{x}P, \tag{4.10}$$

where $\bar{x} = 1 - x$ and x parametrizes the longitudinal momentum fraction so that $0 \leq x \leq 1$.

To evaluate the matrix elements involved in the amplitudes we need to construct the wave function for the pion which is a bound state of quarks. Here we employ the light cone distribution amplitudes for light pseudo-scalar mesons up to the leading twist [64] and so we can define the matrix

$$\langle \pi(P)|\bar{d}(z_2)u(z_1)|0\rangle = \frac{if_\pi}{4}(\slashed{P}\gamma_5) \int_0^1 dx e^{i(xp\cdot z_2 + \bar{x}p\cdot z_1)}\phi_\pi(x), \tag{4.11}$$

where $\phi_\pi(x) = 6x(1-x)$ is the leading twist distribution amplitude for the light meson in the asymptotic limit. After integrating over the momentum fraction x and taking traces over the Dirac structure in the relevant matrix elements the amplitude simplifies to

$$\mathcal{M}_{u+d} = \frac{ge}{2\sqrt{2}}\frac{f_\pi}{4}\frac{|V_{ud}|}{(P\cdot k)}[6P\cdot kg^{\mu\lambda} - 2P_\mu k_\lambda + 2i\epsilon^{\alpha\beta\mu\lambda}k_\alpha P_\beta]\epsilon_\mu^*(k)\epsilon_\lambda(P+k). \tag{4.12}$$

Since we are working in the massless pion limit, $2(P\cdot k) \to m_W^2$ in the frame of the decaying W boson and the total amplitude including all three contributing diagrams is

$$\mathcal{M}_{W+u+d} = \frac{ge}{2\sqrt{2}}|V_{ud}|\frac{f_\pi}{m_W^2}[P\cdot kg^{\mu\lambda} - P_\mu k_\lambda + i\epsilon^{\alpha\beta\mu\lambda}k_\alpha P_\beta]\epsilon_\mu^*(k)\epsilon_\lambda(P+k), \tag{4.13}$$

which we can see is gauge invariant. If we compare this amplitude to the general analysis from Section 4.1, we see that the form factors that stem from the vector and axial-vector

component of the weak charged current is just simply $H_6 = H_2 = \frac{-f_\pi}{m_W^2}$. The decay width that is obtained from the amplitude after the two-body phase space integrations is

$$\Gamma = \frac{\alpha G_F}{24\sqrt{2}} |V_{ud}|^2 m_W^3 \left(1 - \frac{m_\pi^2}{m_W^2}\right)^3 \left(\frac{2f_\pi^2}{m_W^2}\right), \tag{4.14}$$

where $\alpha = e^2/4\pi = 1/137$ and G_F is the fermi constant. Using the numerical values of $m_w = 80.3$ GeV, $f_\pi = 0.132$ GeV, $|V_{ud}| = 0.9$ and the lifetime of the W boson from the PDG we get the branching ratio for the process

$$\mathcal{B}r[W^\pm \to \pi^\pm \gamma] = 3.2 \times 10^{-9}. \tag{4.15}$$

4.3   Amplitude in SCET

We can write out the amplitude in SCET and obtain its factorization. The general lorentz invariant and gauge invariant expression for the $W^\pm \to \pi^\pm \gamma$ decay as seen previously in Section 4.1 is given by

$$\mathcal{M} = -\frac{ge}{2\sqrt{2}} |V_{ud}| [H_2(P \cdot k g^{\mu\lambda} - P_\mu k_\lambda) + iH_6 \epsilon^{\alpha\beta\mu\lambda} k_\alpha P_\beta] \epsilon_\mu^*(k) \epsilon_\lambda (P + k),$$

where H_2 and H_6 correspond to the axial-vector and vector form factors respectively.

If we look at this decay process in a SCET basis, the mass of the decaying W gives us a hard scale M_W. In its rest frame the W boson decays into a hard real photon and a light pion that are back to back carrying about half the rest mass energy (in the limit of a massless pion). The quarks constituting the pion are thus collinear and we can choose the momentum of the photon along a light cone direction. If we parametrize a light cone direction along z say, for the collinear particle $n^\mu = (1, 0, 0, 1)$ and an orthogonal direction $\bar{n}^\mu = (1, 0, 0, -1)$

so that $n^2 = \bar{n}^2 = 0$ and $n \cdot \bar{n} = 2$, we can set the momentum of the particles in the light cone basis to be

$$P^\mu = \frac{M_W}{2} n^\mu$$
$$k^\mu = \frac{M_W}{2} \bar{n}^\mu. \tag{4.16}$$

In this SCET basis, Eq.(4.3) is written as

$$\mathcal{M} = -\frac{ge}{2\sqrt{2}} |V_{ud}| \frac{M_W^2}{4} [H_2(2g^{\mu\lambda} - n_\mu \bar{n}_\lambda) + iH_6 \epsilon^{\mu\lambda\alpha\beta} \bar{n}_\alpha n_\beta] \epsilon_\mu^*(k) \epsilon_\lambda(P + k). \tag{4.17}$$

In fact we can notice that the $n_\mu \bar{n}_\lambda$ term multiplying $\epsilon_\mu^*(k)$ would vanish since in the rest frame of the pion, (and thus in all other frames due to Lorentz invariance), the photon polarization is orthogonal to its momentum and therefore also orthogonal to the back to back pion momentum.

We can now perform a matching at the required order to the operator in the effective theory and obtain the relevant form factors in SCET. At tree level the amplitude can be written from the diagrams in Fig. 4.2.1(b). The pion consists of collinear quarks so the full theory current would match on to operators of the form

$$\mathcal{O} = [\bar{\xi}_{n,P_d} W] \Gamma C(\bar{n} \cdot p, \mu) [W^\dagger \xi_{n,P_u}], \tag{4.18}$$

where C is a hard matching coefficient that is a function of the large collinear momentum and the cut-off scale μ of the effective theory [65]. The C's describe the short distance interactions. The presence of the Wilson lines built out of collinear gluon fields ensures that the operator is invariant under collinear gauge transformations and are required to connect the non-local fields

$$W(y, -\infty) = \mathrm{P} \exp \left[ig \int_{-\infty}^y ds \, \bar{n} \cdot A_n(s\bar{n}) \right]. \tag{4.19}$$
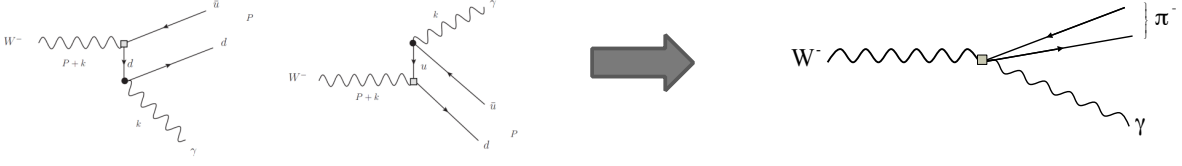
Figure 4.3.1: Matching full theory diagrams to effective diagram at tree level

Using time ordered products of electromagnetic and weak currents and inserting the appropriate quark propagator, we can write out the tree level amplitude for the diagrams in Fig. 4.3.1 as

$$\mathcal{M}_d = \frac{-ige}{2\sqrt{2}} Q_d \langle \pi | [\bar{\xi}_{n,P_d} W] \gamma_\perp^\mu \frac{(x \not{n} + \not{\bar{n}})}{2x M_w} \gamma^\lambda (1-\gamma_5)[W^\dagger \xi_{n,P_u}]|0\rangle \epsilon_\mu^*(k)\epsilon_\lambda(P+k) \quad (4.20)$$

$$\mathcal{M}_u = \frac{-ige}{2\sqrt{2}} Q_u \langle \pi | [\bar{\xi}_{n,P_d} W] \gamma^\lambda (1-\gamma_5)\frac{(-\bar{x} \not{n} - \not{\bar{n}})}{2\bar{x} M_w}\gamma_\perp^\mu [W^\dagger \xi_{n,P_u}]|0\rangle \epsilon_\mu^*(k)\epsilon_\lambda(P+k). \quad (4.21)$$

Here x is the fraction of the longitudinal pion momentum carried by the down quark and only the transverse component of the electromagnetic vertex, $\gamma_\perp^\mu = \gamma^\mu - \frac{n^\mu \not{\bar{n}}}{2} - \frac{\bar{n}^\mu \not{n}}{2}$ is relevant since the photon polarization is orthogonal to its momentum along the light cone. Using the equations of motion for the collinear fields $\not{n}\xi_{n,P} = 0$, $\frac{\not{\bar{n}}\not{n}}{4}\xi_{n,P} = \xi_{n,P}$ we can simplify the amplitude expressions and match their sum onto Eq.(4.3) to obtain the expressions for the form factors

$$H_2 = \frac{i}{M_W^3}\left(\frac{Q_d}{x} - \frac{Q_u}{\bar{x}}\right)\langle \pi|[\bar{\xi}_{n,P_d}W]\not{\bar{n}}(1-\gamma_5)[W^\dagger \xi_{n,P_u}]|0\rangle - \frac{4f_\pi}{M_W^2} \quad (4.22)$$

$$H_6 = \frac{i}{M_W^3}\left(\frac{Q_d}{x} + \frac{Q_u}{\bar{x}}\right)\langle \pi|[\bar{\xi}_{n,P_d}W]\not{\bar{n}}(1-\gamma_5)[W^\dagger \xi_{n,P_u}]|0\rangle. \quad (4.23)$$

The second term in H_2 corresponds to the contribution from the W emitting the photon. In SCET the matrix element can be written in terms of the light cone distribution amplitude for the pion by boosting the expression involving the pion wavefunction defined by Brodsky-Lepage. Defining $C_2 = \frac{Q_d}{x} - \frac{Q_u}{\bar{x}}$, $C_6 = \frac{Q_d}{x} + \frac{Q_u}{\bar{x}}$ and $\Gamma = \not{\bar{n}}\gamma_5$, we obtain the factorization

$$C_{2,6}\langle\pi|[\bar{\xi}_{n,P_d}W]\Gamma[W^\dagger\xi_{n,P_u}]|0\rangle = -if_\pi\bar{n}\cdot P_\pi\int_0^1 C_{2,6}\phi_\pi(x)dx. \qquad (4.24)$$

We can use the leading twist pion distribution amplitude as before and we know $\bar{n}\cdot P = M_W$. After integrating over the momentum fraction we obtain the result $H_2 = H_6 = -\frac{f_\pi}{M_W^2}$ which is the same as the result from PQCD approach at tree level. We therefore have established a factorization formula so that the form factors can be written as a convolution of a hard matching coefficient parametrizing the short distance, with the light-cone pion distribution wavefunction. We expect this factorization to hold at all orders.

4.4   Summary and Further Work

We studied the rare radiative exclusive decay of the W boson into a pion and an energetic photon. We calculated the relevant form factors and obtained a branching ratio for the process at tree level in pQCD and SCET. The enhancement in the branching ratio claimed by [63] was not found at tree level. We showed the factorization of the form factors in the amplitude into a hard matching coefficient and a light cone distribution function at tree level in SCET. We expect such a factorization to occur at higher orders as well and we are calculating the order α_s corrections at one-loop in SCET. We have calculated the one-loop diagrams in pQCD, which include collinear virtual gluons that contribute to the structure dependent part of the amplitude akin to [66]. We can then match them onto the relevant loop diagrams in the effective theory, as shown in Fig. 4.4.1, to the obtain higher order corrections to the transition form factors in SCET.
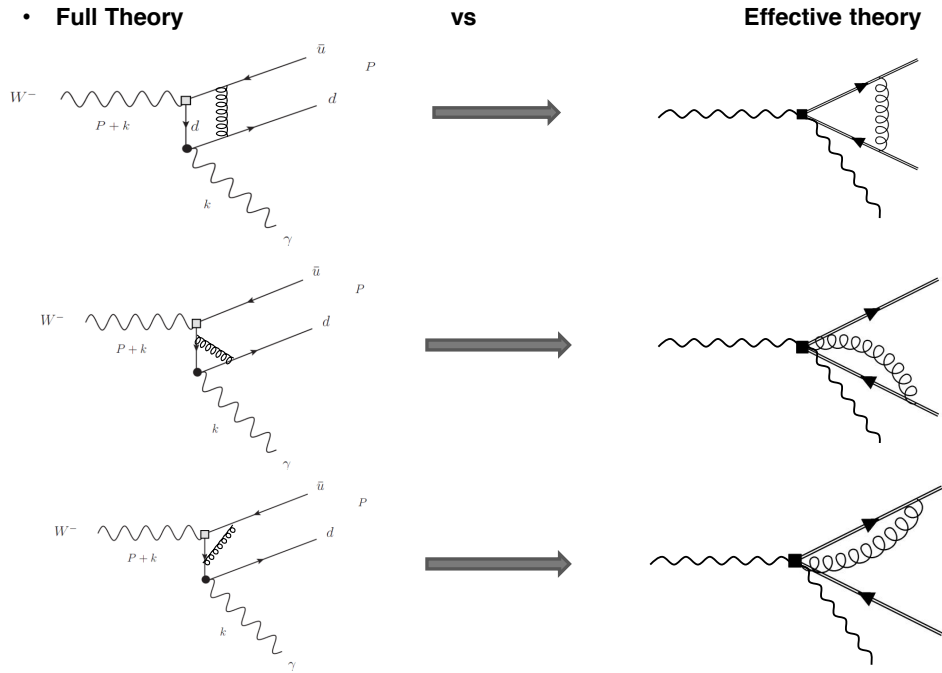
Figure 4.4.1: Matching diagrams from full theory onto effective theory at one-loop

We wish to verify wether the enhancement is an artifact of the constituent quark model being used in [63] or if it might arise from the one-loop diagrams and resummation of any logarithmic terms that arise from the higher order calculations. We also aim to extend the calculations to include the charmed mesons in the decay, such as $W \to D\gamma$.

CHAPTER 5

SUPER-WIMPS IN HEAVY MESON DECAYS

5.1 Weaker than WIMPS

There is evidence that the amount of dark matter (DM) in the universe by far dominates that of the luminous matter. It comes from a variety of cosmological sources such as the rotation curves of galaxies [14], features of CMB [15], gravitational lensing [16] and large scale structures [17]. While the presence of DM is firmly established, its basic properties are still a subject of debate. If dark matter is comprised of some fundamental particle, experimentally-measured properties, such as its relic abundance or production cross-sections can be predicted. Experimental measurements of the abundance $\Omega_{DM}h^2 \sim 0.12$ by the WMAP collaboration [67] can be used to place constraints on the masses and interaction strengths of the DM particles. Indeed, the relation

$$\Omega_{DM}h^2 \sim \langle \sigma_{ann}v_{rel} \rangle^{-1} \propto \frac{M^2}{g^4}, \tag{5.1}$$

with M and g being the mass and the interaction strength associated with DM annihilation, implies that, for a weakly-interacting massive particle (WIMP) of DM, the mass scale should be set around the electroweak scale. Yet, difficulties in understanding of small-scale gravitational clustering in numerical simulations with WIMPs may lead to preference being given to much lighter DM particles. Particularly there has been interest in studying models of light dark matter particles with masses of the keV range [68, 69]. According to Eq. (5.1), the light mass of the dark matter particle then implies a superweak interaction between the dark matter and standard model (SM) sector [70]. Several models with light $\mathcal{O}(\text{keV-MeV})$

DM particles, or super-WIMPs, have been proposed [68, 69].

One of the main features of the super-WIMP models is that DM particles do not need to be stable against decays to even lighter SM particles [68]. This implies that one does not need to impose an ad-hoc Z_2 symmetry when constructing an effective Lagrangian for DM interactions with the standard model fields, so DM particles can be emitted and absorbed by SM particles. Due to their extremely small couplings to the SM particles, experimental searches for super-WIMPs must be performed at experiments where large statistics are available. In addition, the experiments must be able to resolve signals with missing energy [71]. Super-B factories fit this bill perfectly.

In this chapter we focus on bosonic super-WIMP models [68, 69] for dark matter candidates and attempt to constrain their couplings with the standard model through examining leptonic meson decays. The idea is quite straightforward. In the standard model the leptonic decay width of, say, a B-meson, i.e. the process $B \to \ell\bar{\nu}$, is helicity-suppressed by $(m_\ell/m_B)^2$ due to the left-handed nature of weak interactions [72],

$$\Gamma(B \to \ell\bar{\nu}) = \frac{G_F^2}{8\pi}|V_{ub}|^2 f_B^2 m_B^3 \frac{m_\ell^2}{m_B^2}\left(1 - \frac{m_\ell^2}{m_B^2}\right)^2. \tag{5.2}$$

Similar formulas are available for charmed meson D^+ and D_s decays with obvious substitution of parameters. The only non-perturbative parameter affecting Eq. (5.2), the heavy meson decay constant f_B, can be reliably estimated on the lattice [74], so the branching ratio for this process can be predicted quite reliably.

The helicity suppression arises from the necessary helicity flip on the outgoing lepton due to angular momentum conservation as the initial state meson is spinless. The suppression can be overcome by introducing a third particle to the final state that contributes to total angular momentum [38, 39, 40] (see Fig. 5.1.1). If that particle is a light DM candidate, helicity suppression is traded for a small coupling strength of DM-SM interaction. In this case, the charged lepton spectrum of the 3-body $B \to \ell\bar{\nu}_\ell + X$ (with X being the DM
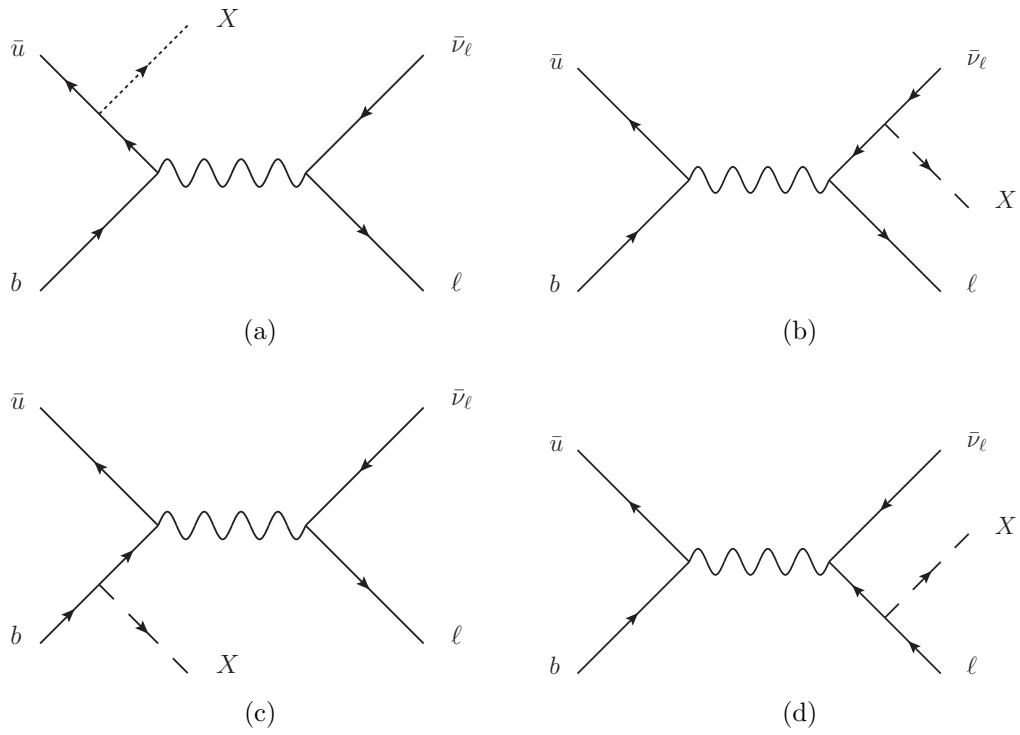
Figure 5.1.1: Diagrams for the super-WIMP emission in $B \to \ell\bar{\nu}_\ell X$. Similar diagrams exist for $D_{(s)}$ decays. Note that the graph (b) is absent for the vector light dark matter particles discussed in section 5.4.

candidate) process will be markedly different from the spectrum of two-body $B \to \ell \bar{\nu}_\ell$ decay. Then, the rate for the process $B \to \ell + \not{E}$, with $\not{E}$ being missing energy, can be used to constrain properties of light DM particles.

We shall consider two examples of super-WIMPs, the "dark photon" spin-1 particle, and a spin-0, axion-like state. The discussion of the vector dark matter effects is similar to a calculation of the radiative leptonic decay [38, 39, 40], i.e. the spin of the added DM particle brings the required unit of angular momentum. In the case of axion-like DM candidate, there is a derivative coupling to the SM allowing the pseudoscalar particle to carry orbital angular momentum and hence overcome helicity suppression as well. As a side note, we add that the models of new physics considered here are very different from the models that are usually constrained in the new physics searches with leptonic decays of heavy mesons [73].

This chapter is organized as follows. In Section 5.2 we examine the decay width for the process $M \to \ell \bar{\nu}_\ell + X$ for $X = a$ being a spin-0 particle. We consider a particular two-Higgs doublet model, taking into account DM-Higgs mixing in Section 5.3. In Section 5.4 we consider constraints on a spin-1 super-WIMP candidate. We conclude in Section 5.5.

5.2   Simple Axion-Like Dark Matter

We consider first an "axion-like" dark matter (ALDM) model, as suggested in [68] and study the tree-level interactions with the standard model fermions. The most general Lagrangian consists of a combination of dimension-five operators,

$$\mathcal{L}_a = -\frac{\partial_\mu a}{f_a} \bar{\psi} \gamma^\mu \gamma_5 \psi + \frac{C_\gamma}{f_a} a F_{\mu\nu} \widetilde{F}^{\mu\nu}, \tag{5.3}$$

where $X = a$ is the DM particle and the coupling constant f_a has units of mass. Taking into account the chiral anomaly we can substitute the second term with a combination of vector

and axial-vector fermionic currents,

$$\mathcal{L}_a = -\left(\frac{1}{f_a} + \frac{4\pi C_\gamma}{f_a \alpha}\right) \partial_\mu a \, \bar{\psi} \gamma^\mu \gamma_5 \psi - i m_\psi \left(\frac{8\pi C_\gamma}{f_a \alpha}\right) a \bar{\psi} \gamma_5 \psi. \tag{5.4}$$

The Feynman diagrams that contribute to the meson decay, for example $B \to \ell \bar{\nu}_\ell + a$, are shown by Fig 5.1.1. The amplitude for the emission of a in the transition $M \to \ell \bar{\nu}_\ell + a$ can be written as

$$\mathcal{A}_{M \to \ell \bar{\nu} a} = \mathcal{A}_\ell + \mathcal{A}_q, \tag{5.5}$$

where $\mathcal{A}_q$, the quark contribution, represents emission of a from the quarks that build up the meson and $\mathcal{A}_\ell$, the leptonic contribution, describe emission of a from the final state leptons.

Let's consider the lepton amplitude first. Here we can parameterize the axial matrix elements contained in the amplitude in terms of the decay constant f_B as

$$\langle 0 | \bar{u} \gamma^\mu \gamma_5 b | B \rangle = i f_B P_B^\mu. \tag{5.6}$$

If the mass of the axion-like DM particle is small ($m_a \to 0$), the leptonic contribution simplifies to

$$\mathcal{A}_\ell = i\sqrt{2} G_F V_{ub} \frac{f_B}{f_a} m_\ell \left(\frac{m_\ell}{2k \cdot p_\ell}[\bar{u}_\ell \, \not{k}(1 - \gamma_5)v_\nu] - [\bar{u}_\ell(1 - \gamma_5)v_\nu]\right). \tag{5.7}$$

Here k is the DM momentum. Clearly, this contribution is proportional to the lepton mass and can, in principle, be neglected in what follows. The contribution to the decay amplitude from the DM emission from the quark current is

$$\mathcal{A}_q = i\langle 0 | \bar{u} \Gamma^\mu b | B \rangle [\bar{u}_\ell \gamma_\mu (1 - \gamma_5)v_\nu] \tag{5.8}$$

where the current $\bar{u}\Gamma^\mu b$ is obtained from the diagrams in Figure 5.1.1 (a) and (c),

$$\Gamma^\mu = \frac{G_F}{\sqrt{2}f_a}V_{ub}\left[\frac{(\not{k}\gamma_5)(\not{k}-\not{p}_u+m_u)\gamma^\mu(1-\gamma_5)}{m_a^2-2p_u\cdot k} + \frac{\gamma^\mu(1-\gamma_5)(\not{p}_b-\not{k}+m_b)(\not{k}\gamma_5)}{m_a^2-2p_b\cdot k}\right]. \quad (5.9)$$

Since the meson is a bound state of quarks we must use a model to describe the effective quark-antiquark distribution. We choose to follow Refs. [75] and [76], where the wave function for a ground state meson M can be written in the form

$$\psi_M = \frac{I_c}{\sqrt{6}}\phi_M(x)\gamma_5(\not{P}_M + M_M g_M(x)). \quad (5.10)$$

Here I_c is the identity in color space and x is the momentum fraction carried by one of the quarks. For a heavy meson H it would be convenient to assign x as a momentum fraction carried by the heavy quark. Also, for a heavy meson, $g_H \sim 1$, and in the case of a light meson $g_L = 0$. For the distribution amplitudes of a heavy or light meson we use

$$\phi_L \quad \sim \quad x(1-x), \quad (5.11)$$

$$\phi_H \quad \sim \quad \left[\frac{(m^2/M_H^2)}{1-x} + \frac{1}{x} - 1\right]^{-2}, \quad (5.12)$$

where m is the mass of the light quark and the meson decay constant is related to the normalization of the distribution amplitude,

$$\int_0^1 \phi_M(x)dx = \frac{f_M}{2\sqrt{6}}. \quad (5.13)$$

The matrix element can then be calculated by integrating over the momentum fraction [76]

$$\langle 0|\bar{q}\Gamma^\mu Q|M\rangle = \int_0^1 dx \, \text{Tr}\left[\Gamma^\mu \psi_M\right]. \quad (5.14)$$

Neglecting the mass of the axion-like DM particle, the decay amplitude in the $B^\pm$ case

simplifies to

$$\mathcal{A}_q = i\frac{\sqrt{3}G_F V_{ub} M_B}{f_a(k \cdot P_B)}\left(M_B \Phi_1^B - m_b \Phi_0^B\right)\left[\bar{\ell}\;\slashed{k}(1 - \gamma_5)\nu\right],\tag{5.15}$$

where m_b is the mass of the b-quark (or, in general, a down-type quark in the decay), and we defined

$$\Phi_n^M = \int_0^1 \frac{\phi_M(x)}{x(1 - x)}x^n dx\tag{5.16}$$

The total decay width is, then,

$$\begin{aligned}\Gamma_{B\to a\ell\nu_\ell} &= \frac{G_F^2 f_B^2 |V_{ub}|^2 M_B^5}{64\pi^3 f_a^2}\left[\frac{1}{6}(2\rho^2 + 3\rho^4 + 12\rho^4 \log\rho - 6\rho^6 + \rho^8)\right.\\ &+ \left. g_B^2\;\Phi(m_b, M_B)^2(1 - 6\rho^2 - 12\rho^4 \log\rho + 3\rho^4 + 2\rho^6)\right],\end{aligned}\tag{5.17}$$

where $\rho \equiv m_\ell/m_B$. Also,

$$\Phi(m_b, M_B) = \frac{m_b \Phi_0 - M_B \Phi_1}{f_B M_B}.\tag{5.18}$$

Note that $\Phi(m_b, M_B) \propto 1/m$, which is consistent with spin-flipping transition in a quark model, which would explain why this part of the decay rate is not proportional to m_ℓ. Similar results for other heavy mesons, like D^+ and D_s^+ are obtained by the obvious substitution of relevant parameters, such as masses, decay constants and CKM matrix elements.

Experimentally, the leptonic decays of heavy mesons are best studied at the e^+e^- flavor factories where a pair of M^+M^- heavy mesons are created. The study is usually done by fully reconstructing one of the heavy mesons and then finding a candidate lepton track of opposite flavor to the tagged meson. The kinematical constraints on the lepton are then used to identify the decays with missing energy as leptonic decay.

In the future super-B factories, special studies of the lepton spectrum in $M \to \ell+$missing energy can be done using this technique to constrain the DM parameters from Eq. (5.17). The lepton energy distributions, which are expected to be quite different for the three-body

Channel (Seen)	Experiment (Maximum)	Standard Model	$f_a^2 R_a(E_0)$ $E_0 = 100$ MeV	$R_{\gamma_s}(E_0')$ $E_0' = 50$ MeV	$R_{\gamma_s}(E_0')$ $E_0' = 100$ MeV	$R_{\gamma_s}(E_0')$ $E_0' = 300$ MeV
$\mathcal{B}\left(B^\pm \to \tau^\pm \bar{\nu}_\tau\right)$	1.7×10^{-4}	7.9×10^{-5}	1.6×10^{2}	4.9×10^{-5}	1.9×10^{-4}	1.9×10^{-3}
$\mathcal{B}\left(D^\pm \to \mu^\pm \bar{\nu}_\mu\right)$	3.8×10^{-4}	3.6×10^{-4}	3.1×10^{3}	4.0×10^{-3}	1.8×10^{-2}	1.7×10^{-2}
$\mathcal{B}\left(D_s^\pm \to \mu^\pm \bar{\nu}_\mu\right)$	5.9×10^{-3}	5.3×10^{-3}	4.6×10^{2}	2.0×10^{-4}	7.8×10^{-4}	6.0×10^{-3}
$\mathcal{B}\left(D_s^\pm \to \tau^\pm \bar{\nu}_\tau\right)$	5.4×10^{-2}	5.1×10^{-2}	6.5×10^{0}	2.1×10^{-5}	8.0×10^{-5}	6.2×10^{-4}
Channel (Unseen)						
$\mathcal{B}\left(B^\pm \to e^\pm \bar{\nu}_e\right)$	$< 1.9 \times 10^{-6}$	8.3×10^{-12}	6.6×10^{7}	4.6×10^{2}	1.8×10^{3}	1.6×10^{4}
$\mathcal{B}\left(B^\pm \to \mu^\pm \bar{\nu}_\mu\right)$	$< 1.0 \times 10^{-6}$	3.5×10^{-7}	1.8×10^{3}	1.1×10^{-2}	4.3×10^{-2}	3.6×10^{-1}
$\mathcal{B}\left(D^\pm \to e^\pm \bar{\nu}_e\right)$	$< 8.8 \times 10^{-6}$	8.5×10^{-9}	3.1×10^{6}	1.9×10^{2}	7.6×10^{2}	7.1×10^{3}
$\mathcal{B}\left(D^\pm \to \tau^\pm \bar{\nu}_\tau\right)$	$< 1.2 \times 10^{-3}$	9.7×10^{-4}	1.0×10^{1}	1.7×10^{-3}	7.7×10^{-3}	6.2×10^{-2}
$\mathcal{B}\left(D_s^\pm \to e^\pm \bar{\nu}_e\right)$	$< 1.2 \times 10^{-4}$	1.2×10^{-7}	9.8×10^{6}	8.6×10^{0}	3.3×10^{1}	2.6×10^{2}

Table 5.2.1: Constraints on f_a from various decays. The last three columns represent possible soft photon pollution of $M \to \ell\bar{\nu}_\ell$ decays for three different values of photon energy cutoff.

decays $B^- \to a\ell^- \bar{\nu}_\ell$ are shown (normalized) in Fig. 5.2.1 for each lepton decay process. However, we can put some constraints on the DM coupling parameters using the currently available data on $M \to \ell\bar{\nu}_\ell$. The experimental procedure outlined above implies that what is experimentally detected is the combination,

$$\begin{aligned}
\Gamma_{\text{exp}}(M \to \ell\bar{\nu}_\ell) &= \Gamma_{\text{SM}}(M \to \ell\bar{\nu}_\ell) + \int_{E<E_0} dE_a \frac{d\Gamma(M \to a\ell\bar{\nu}_\ell)}{dE_a} \\
&= \Gamma_{\text{SM}}(M \to \ell\bar{\nu}_\ell) \left[1 + R_a(E_0)\right],
\end{aligned} \tag{5.19}$$

where E_0 is the energy cutoff that is specific for each experiment. Equivalently, cutoff in q^2 can also be used. In the above formula we defined

$$R_a(E_0) = \frac{1}{\Gamma_{\text{SM}}(M \to \ell\bar{\nu}_\ell)} \int_{E<E_0} dE_a \frac{d\Gamma(M \to a\ell\bar{\nu}_\ell)}{dE_a}. \tag{5.20}$$

Our bounds on the DM couplings from different decay modes are reported in Table 5.2.1 for the cutoff values of $E_0 = 100$ MeV. Note that similar expressions for the leptonic decays of the *light* mesons, such as $\pi \to a\ell\bar{\nu}$ and $K \to a\ell\bar{\nu}$ come out to be proportional to the mass of the final state lepton. This is due to the fact that in the light meson decay the term proportional to g vanishes. Thus, those decays do not offer the same relative enhancement of

the three-body decays due to removal of the helicity suppression in the two-body channel. It is interesting to note that the same is also true for the heavy mesons if a naive non-relativistic constituent quark model (NRCQM), similar to the one used in Refs. [77, 78] is employed. We checked that a simple replacement

$$p_b = \frac{m_b}{m_B} P_B, \qquad p_u = \frac{m_u}{m_B} P_B \qquad (5.21)$$

advocated in [77, 78] is equivalent to use of a symmetric (with respect to the momentum fraction carried by the heavy quark) distribution amplitude, which is not true in general.

Currently, the SM predictions for the $B^- \to \ell^- \bar{\nu}_\ell$ decay for $\ell = \mu, e$ are significantly smaller than the available experimental upper bounds [79, 80], which is due to the smallness of V_{ub} and the helicity suppression of this process. Thus, even in the standard model, there is a possibility that some of the processes $B^- \to \gamma_s \ell^- \bar{\nu}_\ell$, with γ_s being the soft photon , are missed by the experimental detector. Such photons would affect the bounds on the DM couplings reported in Table 5.2.1.

The issue of the soft photon "contamination" of $B^- \to \ell^- \bar{\nu}_\ell$ is non-trivial if model-independent estimates of the contributions are required (for the most recent studies, see [38]). In order to take those into account, the formula in Eq. (5.19) should be modified to

$$\Gamma_{\exp}(M \to \ell \bar{\nu}_\ell) = \Gamma_{\rm SM}(M \to \ell \bar{\nu}_\ell) \left[1 + R_a(E_0) + R_{\gamma_s}(E_0')\right]. \qquad (5.22)$$

In general, the experimental soft photon cutoff E_0' could be different from the DM emission cutoff E_0. Since we are only interested in the upper bounds on the DM couplings, this issue is not very relevant here, as the amplitudes with soft photons do not interfere with the amplitudes with DM emission. Nevertheless, for the purpose of completeness, we evaluated the possible impact of undetected soft photons using NRCQM as seen in [77, 78]. The results are presented in Table 5.2.1 for different values of cutoff on the photon's energy. We present
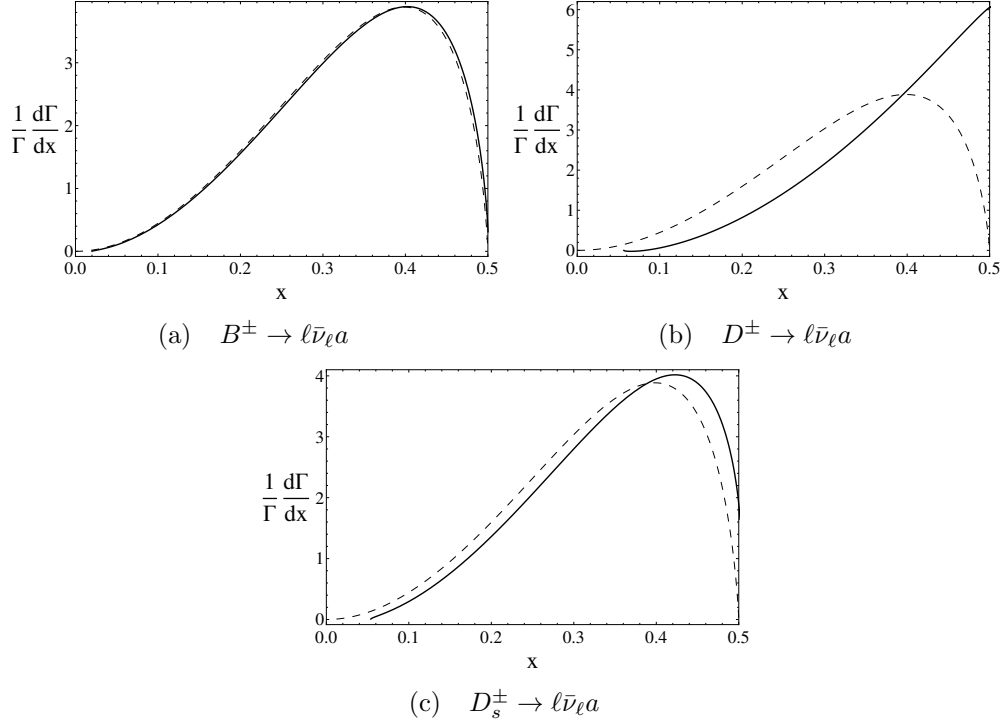
Figure 5.2.1: Normalized electron (dashed) and muon (solid) energy distributions for the heavy $(B^\pm, D^\pm, D_s^\pm)$ meson decay channels. Here $m_a = 0$ and $x = E_\ell / m_B$.

the NRCQM mass parameters in Table 5.2.2 with the decay constants calculated in [81]. The relevant plots for D (D_s) decays can be obtained upon substitution $M_B \to M_{D(D_s)}$, $f_B \to f_{D(D_s)}$, and $V_{ub} \to V_{cd(cs)}$. Note that there is no CKM suppression for D_s decays. In order to bound f_a we use the experimentally seen transitions $B \to \tau\bar{\nu}$, $D_{(s)} \to \mu\bar{\nu}$, and $D_s \to \tau\bar{\nu}$. We note that the soft photon "contamination" can be quite large, up to 10% of the standard model prediction for the two body decay. The resulting fits on f_a can be found in Table 5.2.3. As one can see, the best constraint comes from the $D^\pm \to \mu^\pm \bar{\nu}_\mu$ decay where experimental and theoretical branching ratios are in close agreement.

Quark	Constituent Mass
m_u	335.5 MeV
m_d	339.5 MeV
m_s	486 MeV
m_c	1550 MeV
m_b	4730 MeV

Table 5.2.2: Constituent quark masses [82] used in calculations.

Channel	f_a, MeV
$\mathcal{B}\left(B^{\pm} \to \tau^{\pm}\bar{\nu}_\tau\right)$	12
$\mathcal{B}\left(D^{\pm} \to \mu^{\pm}\bar{\nu}_\mu\right)$	236
$\mathcal{B}\left(D_s^{\pm} \to \mu^{\pm}\bar{\nu}_\mu\right)$	62
$\mathcal{B}\left(D_s^{\pm} \to \tau^{\pm}\bar{\nu}_\tau\right)$	11

Table 5.2.3: Constraint on f_a using the various seen decay channels.

5.3 Axion-like Dark Matter in a Type II Two Higgs Doublet Model

The generic axion-like DM considered in the previous section was an example of a simple augmentation of the standard model by an axion-like dark matter particle. A somewhat different picture can emerge if those particles are embedded in more elaborate beyond the standard model (BSM) scenarios. For example, in models of heavy dark matter of the "axion portal"-type [83], spontaneous breaking of the Peccei-Quinn (PQ) symmetry leads to an axion-like particle that can mix with the CP-odd Higgs A^0 of a two Higgs doublet model (2HDM). For the sufficiently small values of its mass this state itself can play the role of the light DM particle. The decays under consideration can be derived from the $B \to \ell\nu A^0$ amplitude. An interesting feature of this model is the dependence of the light DM coupling upon the quark mass. This means that the decay rate would be dominated by the contributions enhanced by the heavy quark mass. This would also mean that the astrophysical

constraints on the axion-like DM parameters might not probe all of the parameter space in this model.

In a concrete model [83], the PQ symmetry $U(1)_{PQ}$ is broken by a large vacuum expectation value $\langle S \rangle \equiv f_a \gg v_{EW}$ of a complex scalar singlet Φ. As in [84], we shall work in an interaction basis so that the axion state appears in Φ as

$$\Phi = f_a \exp\left[\frac{ia}{\sqrt{2}f_a}\right] \tag{5.23}$$

and A^0 appears in the Higgs doublets in the form

$$\Phi_u = \begin{pmatrix} v_u \exp\left[\frac{i\cot\beta}{\sqrt{2}v_{EW}}A^0\right] \\ 0 \end{pmatrix}, \qquad \Phi_d = \begin{pmatrix} 0 \\ v_d \exp\left[\frac{i\tan\beta}{\sqrt{2}v_{EW}}A^0\right] \end{pmatrix}, \tag{5.24}$$

where we suppress the charged and CP-even Higgses for simplicity and define $\tan\beta = v_u/v_d$ and $v_{EW} = \sqrt{v_u^2 + v_d^2} \equiv \frac{m_W}{g}$. We choose the operator that communicates PQ charge to the standard model to be of the form[1]

$$\mathcal{L} = \lambda \Phi^2 \Phi_u \Phi_d + h.c. \tag{5.25}$$

This term contains the mass terms and, upon diagonalizing, the physical states in this basis are given by [84]

$$a_p = a\cos\theta - A^0\sin\theta \tag{5.26}$$

$$A_p^0 = a\sin\theta + A^0\cos\theta \tag{5.27}$$

where $\tan\theta = (v_{EW}/f_a)\sin 2\beta$. Here a_p denotes the "physical" axion-like state. Thus, the

---

[1]This is the case of the so-called Dine-Fischler-Srednicki-Zhitnitsky (DFSZ) axion, although other forms of the interaction term with other powers of the scalar field Φ are possible [84].

Channel	$f_a(MeV)$ $\tan\beta = 1$	$f_a(MeV)$ $\tan\beta = 5$	$f_a(MeV)$ $\tan\beta = 10$	$f_a(MeV)$ $\tan\beta = 20$
$\mathcal{B}\left(B^{\pm} \to \tau^{\pm}\bar{\nu}_{\tau}\right)$	70	340	357	361
$\mathcal{B}\left(D^{\pm} \to \mu^{\pm}\bar{\nu}_{\mu}\right)$	416	2874	3078	3131
$\mathcal{B}\left(D_s^{\pm} \to \mu^{\pm}\bar{\nu}_{\mu}\right)$	532	1380	1499	1529

Table 5.3.1: Constraint on f_a using the observed decays for various $\tan\beta$s.

amplitude for $B \to \ell\nu a_p$ can be derived from

$$\mathcal{M}(B \to \ell\nu a_p) = -\sin\theta\mathcal{M}(B \to \ell\nu A^0) + \cos\theta\ \mathcal{M}(B \to \ell\nu a) \qquad (5.28)$$

In a type II 2HDM [84, 85], the relevant Yukawa interactions of the CP-odd Higgs with fermions are given by

$$\mathcal{L}_{A^0 f\bar{f}} = \frac{ig\tan\beta}{2m_W}m_d\bar{d}\gamma_5 dA^0 + \frac{ig\cot\beta}{2m_W}m_u\bar{u}\gamma_5 uA^0 \qquad (5.29)$$

where $d = \{d, s, b\}$ refers to the down type quarks and $u = \{u, c, t\}$ refers to the up type quarks. The interaction with leptons are the same as above with $d \to \ell$ and $u \to \nu$.

In the axion portal scenario the axion mass is predicted to lie within a specific range of $360 < m_a \leq 800$ MeV to explain the galactic positron excess [83]. Using the quark model introduced in the previous section we obtain the decay width

$$\begin{aligned}
\Gamma\left(B \to \ell\nu_{\ell}a_p\right) &= \frac{G_F^2|V_{ub}|^2 m_B^3}{256\pi^3\left(f_a^2 + v_{EW}^2\sin^2 2\beta\right)} \\
&\times \left[\cos 2\beta\left(m_u\Phi_1^B + m_b(\Phi_0^B - \Phi_1^B)\right) + 5\left[m_b(\Phi_1^B - \Phi_0^B) + m_u\Phi_1^B\right]\right]^2 \\
&\times \left[12x_a^4\log(x_a) - 4x_a^6 + 3x_a^4 + (\rho - 1)^4(4(\rho - 2)\rho + 1) - 12(\rho - 1)^4\log(1 - \rho)\right]
\end{aligned} \qquad (5.30)$$

Here we defined $x_a = m_a/m_B$, and $\rho = m_\ell/m_B$. If we assume $f_a \gg v_{EW}\sin 2\beta$ we can then provide bounds on f_a as seen in Table 5.3.1. Just like in the previous section, the results for other decays, such as $D_{(s)} \to \ell\bar{\nu}_\ell$, can be obtained by the trivial substitution of masses and

decay constants.

5.4   Light Vector Dark Matter

Another possibility for a super-WIMP particle is a light (keV-range) vector dark matter boson (LVDM) coupled to the SM solely through kinetic mixing with the hypercharge field strength [68]. This can be done consistently by postulating an additional $U(1)_V$ symmetry. The relevant terms in the Lagrangian are

$$\mathcal{L} = -\frac{1}{4}F_{\mu\nu}F^{\mu\nu} - \frac{1}{4}V_{\mu\nu}V^{\mu\nu} - \frac{\kappa}{2}V_{\mu\nu}F^{\mu\nu} + \frac{m_V^2}{2}V_\mu V^\mu + \mathcal{L}_{h'}, \tag{5.31}$$

where $\mathcal{L}_{h'}$ contains terms with, say, the Higgs field which breaks the $U(1)_V$ symmetry, κ parameterizes the strength of kinetic mixing, and, for simplicity, we directly work with the photon field A_μ. In this Lagrangian only the photon A_μ fields (conventionally) couple to the SM fermion currents.

It is convenient to rotate out the kinetic mixing term in Eq. (5.31) with field redefinitions

$$A \to A' - \frac{\kappa}{\sqrt{1-\kappa^2}}V', \qquad\qquad V \to \frac{1}{\sqrt{1-\kappa^2}}V'. \tag{5.32}$$

The mass m_V will now be redefined as $m_V \to \frac{m_V}{\sqrt{1-\kappa^2}}$. Also, both A'_μ and V'_μ now couple to the SM fermion currents via

$$\mathcal{L}_f = -eQ_f A'_\mu \bar{\psi}_f \gamma^\mu \psi_f - \frac{\kappa e Q_f}{\sqrt{1-\kappa^2}} V'_\mu \bar{\psi}_f \gamma^\mu \psi_f, \tag{5.33}$$

where Q_f is the charge of the interacting fermion thus introducing our new vector boson's coupling to the SM fermions. Calculations can now be carried out with the approximate

modified charge coupling for $\kappa \ll 1$,

$$\frac{\kappa e}{\sqrt{1 - \kappa^2}} \approx \kappa e. \tag{5.34}$$

As we can see, in this case the coupling of the physical photon did not change much compared to the original field A_μ, while the DM field V'_μ acquired small gauge coupling κe. It is now trivial to calculate the process $B \to \ell \bar{\nu} V_{DM}$, as it can be done similarly to the case of the soft photon emission in Sect. 5.2. Employing the gauge condition $\epsilon \cdot k = 0$ for the DM fields, the amplitudes become in the limit $m_V \to 0$

$$\begin{aligned}
\mathcal{A}_q &= i\frac{G_F V_{ub} \kappa e \epsilon^{*\alpha}}{6 k \cdot p_B}[A_\alpha^\mu \bar{\ell} \gamma_\mu (1 - \gamma_5)\nu_\ell + B \bar{\ell} \gamma_\alpha (1 - \gamma_5)\nu_\ell + C_\alpha \bar{\ell}(1 - \gamma_5)\nu_\ell, \\
&+ D^\mu \bar{\ell} \sigma_{\mu\alpha}(1 + \gamma_5)\nu_\ell]
\end{aligned} \tag{5.35}$$

with the coefficients

$$\begin{aligned}
A_\alpha^\mu &= \left[3\sqrt{2} f_B - 2\sqrt{3}(\Phi_0^B + \Phi_1^B)\right] k^\mu q^\alpha - 2\sqrt{3}(\Phi_0^B - 3\Phi_1^B)i\epsilon^{\mu\alpha\sigma\rho}k_\sigma q_\rho, \tag{5.36} \\
B &= -\left[3\sqrt{2} f_B - 2\sqrt{3}(\Phi_0^B + \Phi_1^B)\right](k \cdot q) - \frac{3}{\sqrt{2}} f_B m_B^2 \\
&\quad - 2\sqrt{3} g m_B \left[m_2(\phi_0 - 3\phi_1) + 2m_B \phi_1\right], \tag{5.37} \\
C_\alpha &= 3\sqrt{2} f_B m_\ell \frac{q^\alpha k \cdot p_\ell - p_\ell^\alpha k \cdot q}{k \cdot p_\ell}, \tag{5.38} \\
D^\mu &= -3\sqrt{2} i f_B m_\ell \frac{k \cdot q}{k \cdot p_\ell} k^\mu, \tag{5.39}
\end{aligned}$$

and $q = p_\ell + p_\nu$. Again, we fit the parameter κ using the same data as in the axion-like DM case. The results are shown in Figure 5.4.1 where the $D^\pm \to \mu^\pm \bar{\nu}_\mu V$ decay can yield the best bound. Using the best constraint on κ from the $D^\pm \to \mu^\pm \bar{\nu}_\mu V$ decay we can limit the contribution to yet-to-be-seen decays in Table 5.4.2.

As we can see, the constraints on the kinetic mixing parameter κ are not very strong, but could be improved in the next round of experiments at super-flavor factories.
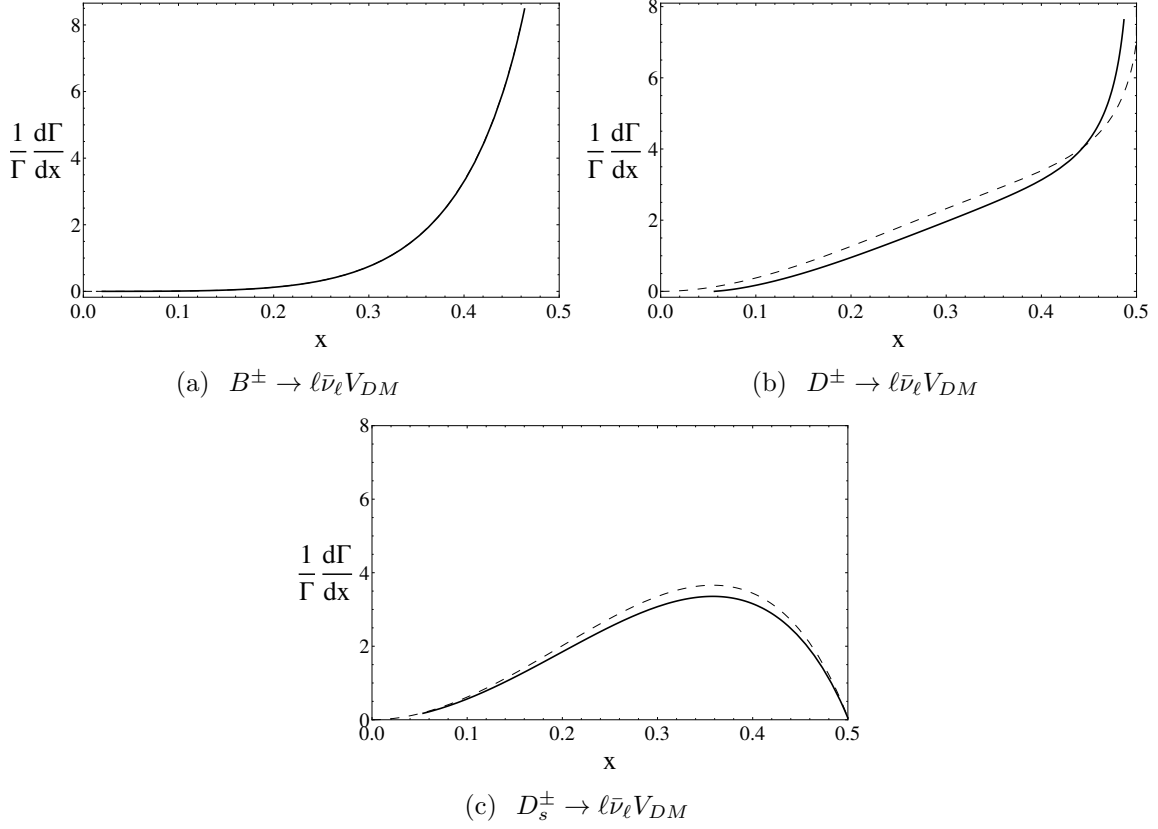
(a) $B^{\pm} \to \ell\bar{\nu}_\ell V_{DM}$

(b) $D^{\pm} \to \ell\bar{\nu}_\ell V_{DM}$

(c) $D_s^{\pm} \to \ell\bar{\nu}_\ell V_{DM}$

Figure 5.4.1: Normalized electron (dashed) and muon (solid) energy distributions for the heavy $\{(B^{\pm}, D^{\pm}, D_s^{\pm}\}$ meson decay channels. Here $m_V = 0$ and $x = E_\ell/m_B$.

Channel	$\kappa^{-2}R_V(E_0)$ $E_0 = 100$ MeV	κ
$\mathcal{B}\left(B^{\pm} \to \tau^{\pm}\bar{\nu}_\tau\right)$	8.8×10^{-3}	≤ 11.6
$\mathcal{B}\left(D^{\pm} \to \mu^{\pm}\bar{\nu}_\mu\right)$	5.7×10^{-1}	≤ 0.31
$\mathcal{B}\left(D_s^{\pm} \to \mu^{\pm}\bar{\nu}_\mu\right)$	5.4×10^{-2}	≤ 1.49
$\mathcal{B}\left(D_s^{\pm} \to \tau^{\pm}\bar{\nu}_\tau\right)$	1.3×10^{-4}	≤ 20.8
$\mathcal{B}\left(B^{\pm} \to e^{\pm}\bar{\nu}_e\right)$	1.8×10^{3}	≤ 11.2
$\mathcal{B}\left(B^{\pm} \to \mu^{\pm}\bar{\nu}_\mu\right)$	1.0×10^{-1}	≤ 4.17
$\mathcal{B}\left(D^{\pm} \to e^{\pm}\bar{\nu}_e\right)$	1.5×10^{3}	≤ 0.83
$\mathcal{B}\left(D^{\pm} \to \tau^{\pm}\bar{\nu}_\tau\right)$	1.8×10^{-4}	≤ 36.4
$\mathcal{B}\left(D_s^{\pm} \to e^{\pm}\bar{\nu}_e\right)$	5.2×10^{2}	≤ 1.37

Table 5.4.1: Constraints on κ using various decay channels. All other values are the same as in Table 5.2.1.

Channel	$\mathcal{B}(\kappa = 0.31)$
$\mathcal{B}\left(B^{\pm} \to e^{\pm}\bar{\nu}_e\right)$	1.4×10^{-9}
$\mathcal{B}\left(B^{\pm} \to \mu^{\pm}\bar{\nu}_\mu\right)$	3.6×10^{-9}
$\mathcal{B}\left(D^{\pm} \to e^{\pm}\bar{\nu}_e\right)$	1.2×10^{-6}
$\mathcal{B}\left(D^{\pm} \to \tau^{\pm}\bar{\nu}_\tau\right)$	1.7×10^{-8}
$\mathcal{B}\left(D_s^{\pm} \to e^{\pm}\bar{\nu}_e\right)$	6.2×10^{-6}

Table 5.4.2: Contributions to various yet-to-be-seen channels using the the fit on κ in Table 5.4.1.

5.5 Results

We considered constraints on the parameters of different types of bosonic super-WIMP dark matter from leptonic decays of heavy mesons. The main idea rests with the fact that in the standard model the two-body leptonic decay width of a heavy meson $M = \{B^{\pm}, D^{\pm}, D_s^{\pm}\}$, or $\Gamma(M \to \ell\bar{\nu})$, is helicity-suppressed by $(m_\ell/m_B)^2$ due to the left-handed nature of weak interactions [72]. A similar three-body decay $M \to \ell\bar{\nu}_\ell X$ decay, which has similar experimental signature, is not helicity suppressed. We put constraints on the couplings of such DM particles to quarks. We note that the models of new physics considered here are very different from the models that are usually constrained in the new physics searches with leptonic decays of heavy mesons [73].

CHAPTER 6

SUMMARY

In this doctoral dissertation we have discussed the possible standard model contributions to select leptonic heavy meson decay modes. We calculated a $1 - 3\%$ increase in $B_s \rightarrow \mu^+\mu^-$ from soft photon contributions through select vector resonances is a nearly model-independent method.

We have analyzed the radiative exclusive W decay $W^\pm \rightarrow \pi^\pm\gamma$ and obtained the form factors involved in describing them at leading order. We calculated the branching ratio for the process and did not notice any enhancement. We established a factorization in SCET for the form factors into a hard matching coefficient and a meson distribution function which would exist at all orders. We are working on improving the calculation at next-to-leading order with the inclusion of 1-loop contributions and resummation of logarithmic terms.

We have computed constraints for two super-WIMP dark matter models from the rare leptonic decays of heavy mesons. While these are not as tight as constraints from new physics, tighter experimental bounds and measurements of particular channels with increased statistics will allow our calculation to be refit more stringently.

REFERENCES

[1] S. L. Glashow, Nucl. Phys. **22**, 579 (1961).

[2] S. Weinberg, Phys. Rev. Lett. **19**, 1264 (1967).

[3] S. L. Glashow and S. Weinberg, Phys. Rev. D **15**, 1958 (1977).

[4] P. W. Higgs, Phys. Rev. Lett. **13**, 508 (1964).

[5] F. Englert and R. Brout, Phys. Rev. Lett. **13**, 321 (1964).

[6] G. S. Guralnik, C. R. Hagen and T. W. B. Kibble, Phys. Rev. Lett. **13**, 585 (1964).

[7] E. C. G. Stueckelberg and A. Petermann, Helv. Phys. Acta **26**, 499 (1953).

[8] D. J. Gross and F. Wilczek, Phys. Rev. Lett. **30**, 1343 (1973).

[9] R. D. Peccei and H. R. Quinn, Phys. Rev. Lett. **38**, 1440 (1977).

[10] F. Wilczek, Phys. Rev. Lett. **40**, 279 (1978).

[11] S. Weinberg, Phys. Rev. Lett. **40**, 223 (1978).

[12] G. Bertone, D. Hooper and J. Silk, Phys. Rept. **405**, 279 (2005) [hep-ph/0404175].

[13] G. Jungman, M. Kamionkowski and K. Griest, Phys. Rept. **267**, 195 (1996) [hep-ph/9506380].

[14] F. Zwicky, Helv. Phys. Acta **6**, 110 (1933); V. C. Rubin and W. K. Ford, Jr., Astrophys. J. 159 (1970) 379-403; V. C. Rubin, N. Thonnard, and W. K. Ford, Jr., Astrophys. J. 238 (1980) 471.

[15] E. Komatsu *et al.*, arXiv:1001.4538 [astro-ph.CO].

[16] A. Refregier, Ann. Rev. Astron. Astrophys. **41**, 645 (2003); Tyson, J. A., Kochanski, G. P., dell'Antonio, I. P. 1998, Astrophys. J. 498, L107

[17] S. W. Allen, A. C. Fabian, R. W. Schmidt and H. Ebeling, Mon. Not. Roy. Astron. Soc. **342**, 287 (2003).

[18] M. R. Buckley, D. Hooper and T. M. P. Tait, Phys. Lett. B **702**, 216 (2011) [arXiv:1011.1499 [hep-ph]].

[19] E. Aprile *et al.* [XENON100 Collaboration], Phys. Rev. Lett. **107**, 131302 (2011) [arXiv:1104.2549 [astro-ph.CO]].

[20] G. Hinshaw, D. Larson, E. Komatsu, D. N. Spergel, C. L. Bennett, J. Dunkley, M. R. Nolta and M. Halpern *et al.*, arXiv:1212.5226 [astro-ph.CO].

[21] E. Fermi, Attempt at a Theory of ?-rays, Il Nuovo Cimento, Vol 11, p 1 (1934); Zeitschrift fur Physik, Vol 88, p 161 (1934)

[22] N. Isgur and M. B. Wise, Phys. Lett. B **237**, 527 (1990); N. Isgur and M. B. Wise, Phys. Lett. B **232**, 113 (1989).

[23] E. Eichten and B. R. Hill, Phys. Lett. B **234**, 511 (1990); E. Eichten and B. R. Hill, Phys. Lett. B **243**, 427 (1990).

[24] B. Grinstein, Nucl. Phys. B **339**, 253 (1990).

[25] T. Mannel, W. Roberts and Z. Ryzak, Nucl. Phys. B **368**, 204 (1992).

[26] J. Gasser and H. Leutwyler, Annals Phys. **158**, 142 (1984); J. Gasser and H. Leutwyler, Nucl. Phys. B **250**, 465 (1985).

[27] S. R. Coleman, J. Wess and B. Zumino, Phys. Rev. **177**, 2239 (1969); C. G. Callan, Jr., S. R. Coleman, J. Wess and B. Zumino, Phys. Rev. **177**, 2247 (1969).

[28] M.B. Wise, Phys. Rev., D45 (1992) 2188; G. Burdman and J. Donoghue, Phys. Lett., B280 (1992) 287; T.M. Yan et al., Phys. Rev. D46 (1992) 1148.

[29] P. L. Cho, Nucl. Phys. B **396**, 183 (1993) [Erratum-ibid. B **421**, 683 (1994)] [hep-ph/9208244].

[30] P. L. Cho and H. Georgi, Phys. Lett. B **296**, 408 (1992) [Erratum-ibid. B **300**, 410 (1993)] [hep-ph/9209239].

[31] E. Golowich, J. Hewett, S. Pakvasa, A.A. Petrov and G.K. Yeghiyan, Phys. Rev. D **83**, 114017 (2011) [arXiv:1102.0009 [hep-ph]], as well as references therein.

[32] R. Aaij *et al.* [LHCb Collaboration], arXiv:1211.2674 [hep-ex].

[33] T. Aaltonen *et al.* [CDF Collaboration], Phys. Rev. Lett. **107**, 191801 (2011).

[34] A. J. Buras, J. Girrbach, D. Guadagnoli and G. Isidori, Eur. Phys. J. C **72**, 2172 (2012) [arXiv:1208.0934 [hep-ph]].

[35] J. Shigemitsu *et al.* [HPQCD Collaboration], PoS **LAT2009**, 251 (2009) [arXiv:0910.4131 [hep-lat]].

[36] A. J. Buras, M. Jamin, M. E. Lautenbacher and P. H. Weisz, Nucl. Phys. B **370**, 69 (1992) [Addendum-ibid. B **375**, 501 (1992)].

[37] D. Melikhov and N. Nikitin, Phys. Rev. D **70**, 114028 (2004) [arXiv:hep-ph/0410146].

[38] D. Becirevic, B. Haas and E. Kou, Phys. Lett. B **681**, 257 (2009) [arXiv:0907.1845 [hep-ph]];

[39] G. Burdman, J. T. Goldman and D. Wyler, Phys. Rev. D **51**, 111 (1995) [hep-ph/9405425].

[40] G. Chiladze, A. F. Falk and A. A. Petrov, Phys. Rev. D **60**, 034011 (1999) [hep-ph/9811405].

[41] Y. G. Aditya, K. J. Healey and A. A. Petrov, Phys. Lett. B **710**, 118 (2012) [arXiv:1201.1007 [hep-ph]].

[42] F. Kruger and D. Melikhov, Phys. Rev. D **67**, 034002 (2003) [arXiv:hep-ph/0208256] ; D. Melikhov and B. Stech, Phys. Rev. D **62**, 014006 (2000) [arXiv:hep-ph/0001113].

[43] M. B. Wise, Phys. Rev. D **45**, 2188 (1992). M. B. Wise, In *Beijing 1993, Proceedings, Particle physics at the Fermi scale* 71-114, and Caltech Pasadena - CALT-68-1860 (93,rec.Jul.) 48 p [hep-ph/9306277].

[44] G. Burdman and J. F. Donoghue, Phys. Lett. B **280**, 287 (1992).

[45] N. Isgur and M. B. Wise, Phys. Rev. D **41**, 151 (1990).

[46] H. Georgi, Phys. Lett. B **240**, 447 (1990). A. F. Falk, B. Grinstein and M. E. Luke, Nucl. Phys. B **357**, 185 (1991).

[47] J. F. Amundson *et al*, Phys. Lett. B **296**, 415 (1992) [hep-ph/9209241].

[48] I. W. Stewart, Nucl. Phys. B **529**, 62 (1998) [hep-ph/9803227].

[49] R. Godang, BaBar Preliminary Results : ICHEP2012.

[50] R. Casalbuoni, *et al*, Phys. Rept. **281**, 145 (1997) [hep-ph/9605342].

[51] T. M. Aliev, N. K. Pak and M. Savci, Phys. Lett. B **424**, 175 (1998) [hep-ph/9710304].

[52] B. Grinstein, M. J. Savage and M. B. Wise, Nucl. Phys. B **319**, 271 (1989). A. J. Buras and M. Munz, Phys. Rev. D **52**, 186 (1995) [hep-ph/9501281].

[53] J. Beringer *et al.* [Particle Data Group Collaboration], Phys. Rev. D **86**, 010001 (2012).

[54] H. Na, *et al*, arXiv:1212.0586 [hep-lat].

[55] A. Axelrod, Phys. Rev. D **29**, 2027 (1984).

[56] C. Quigg, Rev. Mod. Phys. **49**, 297 (1977); R. F. Peierls, T. L. Trueman and L. -L. Wang, Phys. Rev. D **16**, 1397 (1977).

[57] W. J. Marciano, Phys. Rev. D **21**, 2425 (1980).

[58] T. Aaltonen *et al.* [CDF Collaboration], Phys. Rev. D **85**, 032001 (2012) [arXiv:1104.1585 [hep-ex]].

[59] F. Abe *et al.* [CDF Collaboration], Phys. Rev. D **58**, 031101 (1998).

[60] J. Alcaraz *et al.* [ALEPH and DELPHI and L3 and OPAL and LEP Electroweak Working Group Collaborations], hep-ex/0612034.

[61] T. E. W. Group [CDF and D0 Collaborations], arXiv:1204.0042 [hep-ex].

[62] L. Arnellos, W. J. Marciano, Z. Parsa and , Nucl. Phys. B **196**, 378 (1982).

[63] Y. Y. Keum and X. -Y. Pham, Mod. Phys. Lett. A **9**, 1545 (1994) [hep-ph/9303300].

[64] M. Beneke, G. Buchalla, M. Neubert, C. T. Sachrajda and , Nucl. Phys. B **606**, 245 (2001) [hep-ph/0104110].

[65] C. W. Bauer, S. Fleming, D. Pirjol, I. Z. Rothstein and I. W. Stewart, Phys. Rev. D **66**, 014017 (2002) [hep-ph/0202088].

[66] E. Braaten, Phys. Rev. D **28**, 524 (1983).

[67] J. Dunkley et al., (WMAP Collaboration), Astrophys. J. Suppl. 180, 306 (2009).

[68] M. Pospelov, A. Ritz and M. B. Voloshin, Phys. Rev. D **78**, 115012 (2008).

[69] M. Pospelov, A. Ritz and M. B. Voloshin, Phys. Lett. B **662**, 53 (2008).

[70] J. L. Feng, A. Rajaraman, and F. Takayama, Phys. Rev. Lett. 91 (2003) 011302; J. L. Feng, A. Rajaraman, and F. Takayama, Phys. Rev. D68 (2003) 063504; S. Dodelson and L. M. Widrow, Phys. Rev. Lett. 72, 17 (1994); A. D. Dolgov and S. H. Hansen, Astropart. Phys. 16, 339 (2002).

[71] B. Batell, M. Pospelov and A. Ritz, Phys. Rev. D **79**, 115008 (2009); B. Batell, M. Pospelov and A. Ritz, arXiv:0911.4938 [hep-ph]; R. Essig, P. Schuster and N. Toro, Phys. Rev. D **80**, 015003 (2009); R. Essig, R. Harnik, J. Kaplan and N. Toro, Phys. Rev. D **82**, 113008 (2010); A. Badin and A. A. Petrov, Phys. Rev. D **82**, 034005 (2010)

[72] For a recent review of experimental analyses, see, e.g., J. L. Rosner, S. Stone, [arXiv:1002.1655 [hep-ex]].

[73] See, e.g., B. A. Dobrescu and A. S. Kronfeld, Phys. Rev. Lett. **100**, 241802 (2008); M. Artuso, B. Meadows and A. A. Petrov, Ann. Rev. Nucl. Part. Sci. **58**, 249 (2008); A. G. Akeroyd and F. Mahmoudi, JHEP **0904**, 121 (2009).

[74] C. T. H. Davies, C. McNeile, E. Follana, G. P. Lepage, H. Na and J. Shigemitsu, Phys. Rev. D **82**, 114504 (2010).

[75] A. Szczepaniak, E. M. Henley and S. J. Brodsky, Phys. Lett. B **243**, 287 (1990).

[76] G. P. Lepage and S. J. Brodsky, Phys. Rev. D **22**, 2157 (1980).

[77] C. H. Chang, J. P. Cheng and C. D. Lu, Phys. Lett. B **425**, 166 (1998).

[78] C. D. Lu and G. L. Song, Phys. Lett. B **562**, 75 (2003).

[79] D. Asner *et al.* [Heavy Flavor Averaging Group Collaboration], arXiv:1010.1589 [hep-ex].

[80] K. Nakamura et al. (Particle Data Group), J. Phys. G 37, 075021 (2010).

[81] W. Lucha, D. Melikhov and S. Simula, arXiv:1011.3723 [hep-ph].

[82] M. D. Scadron, R. Delbourgo and G. Rupp, J. Phys. G **32**, 735 (2006).

[83] Y. Nomura and J. Thaler, Phys. Rev. D **79**, 075008 (2009).

[84] M. Freytsis, Z. Ligeti and J. Thaler, Phys. Rev. D **81**, 034001 (2010).

[85] G. C. Branco, P. M. Ferreira, L. Lavoura, M. N. Rebelo, M. Sher and J. P. Silva, arXiv:1106.0034 [hep-ph]; A. E. Blechman, A. A. Petrov and G. Yeghiyan, JHEP **1011**, 075 (2010).

ABSTRACT

WEAK DECAY STUDIES FROM AN EFFECTIVE THEORY STANDPOINT

by

ADITYA YECHAN GUNJA

August 2014

Advisor: Dr. Alexey A. Petrov

Major: Physics

Degree: Doctor of Philosophy

In this doctoral dissertation I discuss the phenomenology of some weak interaction decays using a model independent approach by employing effective field theories. I discuss the soft photon contribution and background effect to the rare dimuonic decay of the neutral B meson. I also study some radiative exclusive W boson decays in the standard model in the context of pQCD and SCET. Additionally I invoke leptonic decays of charged mesons to constrain two general models of light dark matter.

AUTOBIOGRAPHICAL STATEMENT

EDUCATION
2008 - 2014 : Ph.D. Physics,   Wayne State University, MI, USA
                 Theoretical Particle Physics
2003 - 2006 : B.Sc (Hons) Physics,   St.Stephens College, New Delhi, India

PROFESSIONAL EXPERIENCE
2009 - 2014 : Graduate Research Assistant
     Dept. of Physics and Astronomy, Wayne State University, MI, USA
2007 - 2009 : Graduate Teaching Assistant
     Dept. of Physics and Astronomy, Wayne State University, MI, USA

ACADEMIC HONORS
2013-2014 : Frank Knoller Fellowship, Wayne State University, MI, USA

PROFESSIONAL TRAINING
2012 : Theoretical Advanced Study Institute (TASI), University of Colorado, Co, USA
2011 : Pre-SUSY Summer school, University of Chicago, IL, USA
Member : American Physical Society

ACADEMIC ACTIVITY
2014 : Phenomenology 2014 Symposium, University of Pittsburgh, PA, USA
2013 : Phenomenology 2013 Symposium, University of Pittsburgh, PA, USA
2012 : Ohio Section APS, Wayne State University, MI, USA
2012 : Phenomenology 2012 Symposium, University of Pittsburgh, PA, USA
2010 : MCTP Spring Symposium on Higgs physics, University of Ann Arbor, MI, USA
2009 : Meeting of the Division of Particles and Fields of APS, Wayne State University, MI, USA

PUBLICATIONS

Faking $B_s \to \mu^+\mu^-$
     Y. G. Aditya, K. J. Healey and A. A. Petrov, arXiv:1212.4166 [hep-ph].

Searching for super-WIMPs in leptonic heavy meson decays
     Y. G. Aditya, K. J. Healey and A. A. Petrov, Phys. Lett. B **710**, 118 (2012)
     [arXiv:1201.1007 [hep-ph]].

CONFERENCE PRESENTATIONS

Exclusive W decay in Effective Field Theory
     Phenomenology 2014 Symposium, May 2014, University of Pittsburgh

Searching for super-WIMPs in leptonic heavy meson decays
     Ohio Section APS Meeting, fall 2012, Wayne State University

Searching for super-WIMPs in leptonic heavy meson decays
     Phenomenology 2012 Symposium, May 2012, University of Pittsburgh